Constraining the Ediacaran-Cambrian boundary in South China using acanthomorphic acritarchs and *Plaeopascichnus* fossils

Kenneth Hugh O'Donnell

Thesis submitted to the faculty of Virginia Polytechnic Institute and State University in partial fulfillment of the requirements for the degree of

Master of Science
In
Geosciences

S. Xiao, Committee Chair
Kenneth A. Eriksson
Patricia E. Dove

May 7, 2013
Blacksburg, VA

Keywords: Biostratigraphy; Heliosphaeridium; Palaeopascichnus; acritarchs; acanthomorphic; Yanjiahe; Liuchapo; Niutitang; Ediacaran; Cambrian; South China

Constraining the Ediacaran-Cambrian boundary in South China using acanthomorphic acritarchs and *Palaeopascichnus* fossils

Kenneth O'Donnell

ABSTRACT

The Ediacaran-Cambrian boundary is arguably the most critical transition in Earth history. This boundary is currently defined by the GSSP (Global Stratotype Section and Point) at Fortune Head (Newfoundland, Canada) at a point that was once regarded as the first appearance of the branching trace fossil *Treptichnus pedum*. However, *T. pedum* has been subsequently found below the GSSP, and its distribution is largely restricted to sandstone facies where chemostratigraphic correlation tools are difficult to apply. Thus, the stratigraphic value of the Fortune Head GSSP has come under scrutiny, and there is a need to search for an alternative definition of this boundary using other biostratigraphic criteria. Investigations of acanthomorphic acritarchs in basal Cambrian strata of South China suggest that these microfossils may provide an appropriate biostratigraphic marker for the Ediacaran-Cambrian boundary, because of their wide distribution in chert-phosphorite layers intercalated with carbonates and shales, thus allowing their biostratigraphic occurrences to be calibrated with small shelly fossil (SSF) biostratigraphy and carbon isotope chemostratigraphy. Acanthomorphic acritarchs of the *Asteridium-Heliosphaeridium-Comasphaeridium* (AHC) assemblage zone have been identified at 11 localities in chert-phosphorite layers in the basal Cambrian Yanjiahe, Liuchapo, and Niutitang formations. These localities span a 300 km transect in South China, with depositional environments varying from a shallow carbonate shelf, to an outer shelf-slope transition and an open ocean slope-basin. The Ediacaran-Cambrian boundary can be bracketed between basal Cambrian AHC assemblage and the upper Ediacaran fossils, *Horodyskia minor* and *Palaeopascichnus jiumenensis* (HmPj assemblage zone), which occur in the lower Liuchapo

Formation. There is no stratigraphic overlap between the AHC and HmPj assemblage zones. Available data show that the AHC assemblage zone is in close stratigraphic proximity with the basal Cambrian SSFs and a negative $\delta^{13}C$ excursion near the Ediacaran-Cambrian boundary. Thus, in South China, the first occurrences of AHC assemblage microfossils and last occurrences of HmPj fossils can effectively "bookend" the Ediacaran-Cambrian boundary to fine-scale resolution (down to 0.5 m in present study) in the Yanjiahe and Liuchapo formations. We propose that the AHC assemblage can be used to redefine the Ediacaran-Cambrian boundary and this proposal should be tested with detailed acanthomorph biostratigraphy beyond South China.

Table of Contents

Table of Figures

Introduction

The Ediacaran-Cambrian transition represents the most significant transition in Earth history, with rapid, drastic changes in ocean chemistry and rapid diversification of biomineralizers, burrowing organisms, and planktonic and nektonic forms. Definition of Cambrian strata is essential for understanding the tempo and mode of environmental and ecological changes at this critical transition. Traditionally, stratigraphic subdivision relies on the first appearance of widely distributed and easily identifiable fossil taxa. To select the Cambrian GSSP, the first appearance of the trace fossil *Treptichnus pedum* at Fortune Head in Newfoundland of Canada was used (Landing, 1994; Narbonne et al., 1987). *Treptichnus pedum* is a burrow with multiple branching probes, probably made by priapulid animals (Vannier et al., 2010). It has a world-wide distribution (Seilacher, 2007) and broad environmental tolerance (Buatois et al., 2013), and it signifies complex burrowing and undermat mining behaviors (Seilacher, 2007), making them a preferred choice to define the Ediacaran-Cambrian boundary (Landing, 1994; Narbonne et al., 1987).

However, *T. pedum* has recently come under question as a reliable biostratigraphic marker. In 2001, *T. pedum* was discovered several meters below the GSSP at Fortune Head, Newfoundland (Fig. 1A), overlapping Ediacaran fossil assemblages containing *Palaeopascichnus delicatus* and *Harlaniella podolica* (Gehling et al., 2001). Treptichnid fossils very similar to *T. pedum* have overlapping stratigraphic ranges with the upper Ediacaran fossil *Cloudina* in Iberia and Namibia (Jensen, 2003; Jensen et al., 2000). Additionally, Seilacher (2007) states that "*Treptichnus pedum* has lately been found in association with the last vendobionts in Australia and Namibia", although illustrations have not been provided. Furthermore, different *Treptichnus* ichnospecies exhibit significant variability (Fig. 1) and

transitional forms between different time periods and physical environments (Seilacher, 2007), making the precise identification of *T. pedum* problematic. More critically, some argue that *T. pedum* has an environmentally controlled distribution and is restricted to shallow marine habitats and transgressive regimes (Geyer, 2005), and its restricted occurrences in sandstone facies (Buatois et al., 2013; Wilson et al., 2012) means that the first appearance of *T. pedum* cannot be precisely calibrated against carbon isotope chemostratigraphy and biostratigraphy based on small shelly fossils and acanthomorphic (spiny) acritarchs. Carbon isotope chemostratigraphy reveals a globally occurring large negative anomaly at the base of Cambrian carbonate successions that is roughly coincident with the first occurrence of Cambrian small shelly fossils (SSFs) (Maloof et al., 2010). SSFs represent the first widespread biomineralization of calcitic and phosphatic skeletons near the base of the Cambrian System, but they typically only occur mainly in phosphatic carbonates. Thus, the correlation power of *T. pedum* is limited to siliciclastic successions, whereas chemostratigraphic and SSF-based biostratigraphic markers have been used independently to define and correlate the Ediacaran-Cambrian boundary in carbonate-dominated successions (Maloof et al., 2010; Steiner et al., 2007).

SSFs have been suggested for regional and global correlation of the Ediacaran-Cambrian boundary (Khomentovskii and Karlova, 2005; Qian et al., 2001; Steiner et al., 2007; Zhu et al., 2003). However, SFF occurrences have been shown to be controlled by facies and taphonomic biases (Porter, 2004), and their stratigraphic distribution in classical sections in southeastern Siberia is plagued by a major unconformity (Knoll et al., 1995). There are also major inconsistencies between SSF-based biostratigraphy and $\delta^{13}C$ chemostratigraphy (Maloof et al., 2010). Thus, although SSFs are useful in regional correlation, much work remains to be done to test the feasibility of using a SSF species to define the Ediacaran-Cambrian boundary.

Although the problem of correlating carbonate with siliciclastic successions can be alleviated to a degree by examining successions with mixed lithologies (Corsetti and Hagadorn, 2000). Mixed lithologies necessarily mean greater environmental fluctuations and, consequently, the facies controlled distribution of *T. pedum* (Geyer, 2005; Wilson et al., 2012) would have a stronger impact on its stratigraphic ranges and limit its biostratigraphic significance. The limitations of *T. pedum* prompt the search for alternative biostratigraphic marker for the Ediacaran-Cambrian boundary.

Horodyskia and Palaeopascichnus, the HmPj biozone

The fossils, *Horodyskia* Yochelson and Fedonkin (2000) and *Palaeopascichnus* Palij (1976), are two well-studied Proterozoic genera that may help to constrain the Ediacaran-Cambrian boundary in South China, with high potential for global correlation. The genus *Horodyskia* was first found by Horodyski (1982) in the Mesoproterozoic Appekuny Formation (~1443 ± 7 Ma) of the Belt Supergroup in Montana, and later systematically described as a body fossil by Yochelson and Fedonkin (2000). It has been suggested to represent either an algal fossil (Grey and Williams, 1990) or early colonial eukaryotes (Fedonkin and Yochelson, 2002; Yochelson and Fedonkin, 2000). The genus *Horodyskia* has a cosmopolitan distribution and long stratigraphic duration, ranging from the Mesoproterozoic of Australia (Grey and Williams, 1990) to the Ediacaran of Lesser Himalaya (Mathur and Srivastava, 2004) and South China (Dong et al., 2008). It is characterized by a "string-of-beads" structure, in which uniserially arranged spheroids of nearly equal size are joined by a filament, with the entire string surrounded by a sheath, typically preserved as a quartz-rich halo when it occurs (Dong et al., 2008). Though the

genus *Horodyskia* has a long stratigraphic range, *H. minor* is well-constrained, known only from upper Ediacaran strata of South China.

The genus *Palaeopascichnus* was first described as an ichnofossil by Palij et al. (1979) and later as a meandering trace fossil (Jenkins, 1995). It has subsequently been demonstrated as a body fossil (Jensen, 2003), based on aggregation and subdivision of palaeopascichnid strands, as well as seemingly gradational relationships with other known body fossils, including *Neonereites*, *Yelovichnus*, and the metaphyte *Orbisiana*, and a lack of evidence for meandering movement of limbs. The genus has since been suggested to represent giant protists (Seilacher et al., 2003), and Dong et al. (2008) have compared both *Palaeopascichnus* to agglutinated foraminifers. It is known exclusively from Ediacaran sedimentary successions in South China (Dong et al., 2008), East European Platform (Palij, 1976), Newfoundland (Landing, 1994), and Australia (Gehling et al., 2000). It exhibits a similar form to *Horodyskia*, but instead has uniserially arranged meniscate discs that are joined by a central filament and surrounded by a quartz-rich halo (Dong et al., 2008). In South China, silicified fossils of the palaeopascichnid *P. jiumenensis* (Dong et al., 2008), have been observed as sinuous strings of meniscate plates that are 0.3 to 1.0 mm wide and 0.9 to 5.0 mm long. It is distinguished from other palaeopascichnid species by its smaller size, lack of branched segments, the presence of a spherical terminal segment, and presence of a quartz halo surrounding the fossil. One species, *Palaeopascichnus delicatus*, comprises part of an important Ediacaran biostratigraphic assemblage zone below the current Cambrian GSSP at Fortune Head, and at sections in Siberia. The affinity between the two forms has not been explored, but there is great potential for global correlation of Ediacaran strata using *Palaeopascichnus*.

Acanthomorphic acritarchs

Recognized as a potentially important biostratigraphic tool in Ediacaran and Cambrian strata, acritarchs are an enigmatic, diverse group of organic-walled, acid-resistant microfossils (Montenari and Leppig, 2003). Despite the 3.2 Ga geological history of the group (Javaux et al., 2010), its morphological diversity varies widely through the Neoproterozoic and Paleozoic climatic events, with a significant increase in abundance and diversity occurring at the base of the Cambrian Period (Huntley et al., 2006; Knoll, 1994; Moczydlowska, 2011). Of particular importance to recognizing the basal Cambrian System in South China is the *Asteridium-Heliosphaeridium-Comasphaeridium* (AHC) assemblage zone (Yao et al., 2005), comprising a group of acanthomorphic acritarchs (*A. tornatum*, *H. ampliatum*, *C. annulare*) and co-occurring with tubular putative metazoans (*Megathrix longus*). The AHC zone has been regionally correlated in South and Northwest China (Dong et al., 2009; Yao et al., 2005) and globally correlated to acritarch assemblages of the Eastern European Platform (Moczydłowska, 1991; Yao et al., 2005) and Lower Tal Formation of India (Tiwari, 1999). The AHC assemblage zone has also been correlated to the SSF I and SSF II horizons (*Anabarites trisulcatus-Protohertzina anabarica* and *Paragloborilus* subglobosus-*Purella squamulosa* SSF zones, respectively) in South China, meaning the base of the AHC assemblage zone may be near the base of the SSF assemblage zones (Yao et al., 2005).

For consistent and reliable identification of basal Cambrian strata, the present study proposes the use of Cambrian acanthomorphic (spiny) acritarchs. In the present study, the biostratigraphic occurrences of Ediacaran microfossils and early Cambrian acanthomorphic acritarchs are correlated at 11 localities across South China (Fig. 2). The goal of this study is to,

1) evaluate the consistency of key fossils across facies and depositional environments along a carbonate shelf to basin transition, 2) assess the possibility of using AHC and HmPj to bracket the Ediacaran-Cambrian boundary in South China, and 3) explore the potential of using the first appearance of a species in the ACH assemblage to redefine the Ediacaran-Cambrian boundary.

Geological Setting

The South China Block comprises the Yangtze and Cathaysia cratons (Fig. 2), which were joined during the early Neoproterozoic assembly of the supercontinent Rodinia (~850-1100 Ma) (Li et al., 2008; Zhao and Cawood, 2012). Between 830 and 750 Ma, South China was separated from Rodinia during supercontinental disassembly (Li et al., 2008; Zhao and Cawood, 2012), resulting in the formation of a southeast-facing passive continental margin. By the Ediacaran Period, the South China Block was completely separated from the supercontinent and developed into a carbonate platform on a passive continental margin (Fig. 3). Shelf facies comprise mixed dolomites and shales of the Ediacaran Doushantuo and Dengying formations that are disconformably overlain by Cambrian strata, comprising carbonates and shales of the Yanjiahe Formation and black shales of the Shuijingtuo Formation. In the slope and basin, strata are composed of basinal black shales of the Doushantuo Formation, overlain by silicified shales of the Liuchapo Formation and basinal black shales of the Niutitang Formation (Fig. 4).

Shelf carbonates of the Doushantuo Formation (ca. 635-551 Ma) (Condon et al., 2005) was deposited in a shelf-lagoonal system on a passive continental margin (Jiang et al., 2011), that developed into a shallow subtidal to peritidal platform during the deposition of Dengying limestones and dolomites. Subaerial exposure features, such as dissolution breccias and paleokarst, are documented at the top of the Denying in South China (Siegmund and Erdtmann, 1994).

The Yanjiahe Formation disconformably overlies the Dengying Formation, consisting of interbedded shelf carbonates, gray to black shale, and cm- to dm-scale black, organic-rich chert layers (Guo et al., *in press*), that were deposited during a marine transgression in a carbonate ramp setting. The inner shelf is composed almost entirely of limestone and dolomite that gradually increases in phosphoritic chert and shale content vertically and towards the shelf edge. It has been previously subdivided into five informal members based on lithostratigraphy (Guo et al., *in press*). The first and lowest member is represented by interbedded silty dolostone and chert, with *Micrhystridium*-like, acanthomorphic acritarchs occurring several meters above the base (Ding et al., 1992; Guo et al., *in press*). The second member is defined by phosphatic intraclastic dolomitic wackestones and packstones, containing the first SSF assemblage (*A. trisulcatus-P. anabarica*) and AHC microfossils. The third member consists of grey mudstone-wackestone interbedded with silty shale, containing the SSF *Purella antiqua*. The fourth member contains carbonaceous limestones and the fifth and uppermost member, grey intraclastic limestones containing *Aldanella yanjiaheensis* (Guo et al., *in press*). The Ediacaran-Cambrian boundary is inferred to occur within the Yanjiahe Formation, near the first occurrence of *A. trisulcatus-P. anabarica* and AHC assemblages, as well as a negative $\delta^{13}C$ isotope excursions within the lower Yanjiahe Formation (Ishikawa et al., 2008; Jiang et al., 2012).

The Shuijingtuo Formation represents a subsequent major marine transgression, depositing basinal black shale facies on top of platform carbonates (Wang et al., 2012b). The Shuijingtuo can be split into two informal members: a lower black shale with interbedded and nodular limestone, and an upper unit of silty shale and argillaceous limestone (Li and Holmer, 2004). In the lower Shuijingtuo Formation, eodiscoid trilobites (Li et al., 2012), lingulid

brachiopods (Li and Holmer, 2004), and bradoriids (Li et al., 2004) corresponding to Cambrian Stage 2 strata indicate a maximum age of approximately 520 Ma.

In the slope to basin transition, black shales of the Doushantuo Formation underlie silicified black shales of the Liuchapo Formation. The Liuchapo Formation was first established in central Hunan based on its characteristic siliceous lithology (Wang and Pien, 1949) and has been regarded as Ediacaran sediments, equivalent in age to the Dengying Formation (Zhu et al., 2003), although some researchers have proposed that the Liuchapo Formation is partly Cambrian in age based on limited chemostratigraphic data (Chen et al., 2009). It comprises silicified organic-rich black shale interbedded with infrequent silt and carbonate beds. Equivalent strata have been named as the Piyuancun Formation in southern Anhui and the Laobao Formation in northern Guangxi (Dong et al., 2012; Zhu et al., 2003). The Liuchapo Formation interfingers the Dengying Formation, and overlies Doushantuo black shales in basinal settings. Though algal fossils are rarely observed within the Liuchapo Formation (Steiner et al., 1992; Steiner, 1994), a lack of detailed biostratigraphic analysis has limited efforts to constrain the Ediacaran-Cambrian boundary in relation to the Liuchapo Formation. Based on radiometric age dates in the underlying and overlying Doushantuo and Niutitang formations, its age is constrained between 551 Ma (Condon et al., 2005) and 532.3 ± 0.7 Ma (Jiang et al., 2009), rendering the Ediacaran-Cambrian boundary possibly within the Liuchapo Formation. Such a view is supported by a report of the early Cambrian *Kaiyangites* SSF in the uppermost Liuchapo Formation of central Guizhou Province (Qian and Yin, 1984). High-resolution biostratigraphic data may properly augment existing geochemical and lithostratigraphic data to constrain the boundary within the Liuchapo Formation.

Overlying the Dengying Formation in outer shelf facies or the Liuchapo Formation in slope to basinal facies, the Niutitang Formation (and its equivalent units) represents a major marine transgression with the deposition of black shale and contains a lower silicified phosphoritic layer that is below metalliferous ore-rich layer (Ni-Mo-PGE) close to its base (Wang et al., 2012b; Zhang et al., 2008). The Niutitang Formation is recognized as part of the Lower Cambrian "black rock series," of South China, and is stratigraphically equivalent to the Shiyantou Formation in Yunnan, Shuijingtuo Formation in Hubei, Xiaoyanxi Formation in Hunan, Hetang Formation in Guizhou, and Guojiaba Formation in Sichuan Province (Steiner et al., 2005; Wang et al., 2012b). The Niutitang Formation can be subdivided into four informal units. The lowermost unit is recognized as a basal phosphoritic chert that occurs within the first meter of the lower Niutitang boundary. This unit is observed in Hunan provinces and has been noted to contain sparse microfossils and SSF (Steiner et al., 2001; Zhang et al., 2001). Potential for biostratigraphic correlation exists, though detailed study of fossil occurrences in the lower phosphorite bed has not been conducted. An organic-rich metalliferous Ni-Mo-PGE sulfide ore layer in the lower Niutitang Formation about 2 m above the base, serves as a laterally persistent marker bed for regional correlation of the Niutitang. This ore layer can be used to distinguish between upper Niutitang strata, with well-defined biostratigraphy, and lower Niutitang strata comprising basal phosphorite and shales, which are not as well-studied. The upper Niutitang comprises carbonaceous "stone coal" beds containing articulated hexactinellid and demosponge fossils. In addition to sponges, exceptional "Burgess-shale type" preservation of archaeocyathians, trilobites, bradoriids, and brachiopods is observed (Peng and Babcock, 2001; Zhang et al., 2008). A volcanic tuff layer has been radiometrically dated to be approximately 532.3 ± 0.7 Ma (Jiang et al., 2009).

In the present study, field sampling of strata focuses on sampling across wide depositional environments on the Yangtze carbonate shelf to basin transition in South China (Fig. 2). Phosphoritic chert of the Yanjiahe Formation, siliceous rocks of the Liuchapo Formation, and the basal Niutitang phosphorite bed are sampled because exquisitely preserved acritarch fossils have been frequently associated with cherts and phosphorites (Dong et al., 2009; Guo et al., *in press;* McFadden et al., 2009; Tiwari, 1999; Yao et al., 2005). Sampling of the Yanjiahe, Liuchapo, and Niutitang formations at multiple sections allows for increased facies coverage, ranging from a shallow carbonate shelf to basinal black shale facies.

Method and Material

523 samples of black phosphoritic cherts and siliceous sediments were collected, with stratigraphic heights recorded, from 15 measured sections along a 300-km north-south transect (Fig. 2). Microfossils of the AHC and HmPj assemblage were found at 11 sections. Sampled strata focused on the Yanjiahe Formation (shelf carbonates intercalated with phosphorites and shales), Liuchapo Formation (outer shelf to basin black siliceous rocks), and the lowermost Niutitang Formation (outer shelf to shelf slope black shales with basal phosphorites). These formations comprise uppermost Ediacaran and lowermost Cambrian successions during early Cambrian transgression on a carbonate shelf ramp system.

Samples from the Yanjiahe Formation are dominantly nodular and bedded phosphoritic cherts, representing silicified carbonates and silty mudstones. The Yanjiahe was sampled at Baiguotang, Jijiapo, Jiuqunao, Hezi'ao, and Wangzishi sections (Appendix 1-5). The Niutitang Formation was at the Ganziping, Sancha, and Daping sections (Appendix 6-8), representing outer shelf, slope, and basinal facies. Samples were collected from the Liuchapo Formation at

Taoying, Siduping, Xugongping, Louyixi, Longbizui, Yanwutan, Jianxincun (Appendix 9-15), representing slope and basinal facies. Among these sampled sections, carbon isotope chemostratigraphic data have been published for the Jijiapo, Jiuqunao, Longbizui, and Yanwutan sections (Compston et al., 1992; Guo et al., *in press;* Guo et al., 2007; Jiang et al., 2012; Wang et al., 2012a), allowing a direct comparison of biostratigraphic with chemostratigraphic data. Radiometric ages have been published from the Doushantuo Formation at Jiuqunao (Condon et al., 2005) and the Niutitang Formation tuffaceous ash bed at the Taoying section (Jiang et al., 2009).

Thin section analysis of samples was conducted using an Olympus BX51 petrographic microscope. Abundances of microfossils were recorded semi-quantitatively (rare = 1 individual; common = 2–7 individuals; abundant = 8+ individuals in a 24×36 mm thin section). Stratigraphic columns are constructed to record the occurrence and abundance of microfossils. Fossils are grouped among AHC acritarchs, HmPj assemblage taxa, tubular microfossils (*Megathrix longus*), SSFs, and stratigraphically non-diagnostic taxa. Stratigraphic occurrences of AHC acritarchs are calibrated against Cambrian SSFs and δ13C chemostratigraphic data to constrain the Ediacaran-Cambrian boundary. Lithological description of carbonate thin sections follows Dunham (1962). Thin sections are reposited at the Department of Geosciences, Virginia Polytechnic Institute, Blacksburg, VA.

Lithostratigraphy

Shelf to basin correlation of Ediacaran and lower Cambrian strata is displayed in Fig. 4. Individual stratigraphic columns of each locality with lithologic information and fossil distributions can be found in Appendix 1-15.

Yanjiahe Formation

The Yanjiahe Formation is dominated by interbedded limestones and dolostone, with minor amounts of shale and chert (Fig. 4; Appendix 1-5). In the present study, the Yanjiahe can be divided into five informal lithologic units. The lowermost unit comprises 6.8-11.5 m of clay- and silt-rich massive dolomitic mudstones and wackestones (Fig. 5A). This unit is observed at Jijiapo, Jiuqunao, and Hezi'ao (Appendix 2-4). It contains phosphatic grains (< 300 μm) occurring with sparse peloids. It has low organic content and bears no diagnostic microfossils or skeletal fragments. Previous studies note *Micrhystridium*-like acritarchs in the lowermost Yanjiahe (Ding et al., 1992), but *Micrhystridium*-like forms are not observed near the base of the Yanjiahe at Hezi'ao.

Unit two occurs directly above unit one, measuring approximately 7.5 to 14 m in thickness. It is defined by silicified phosphatic dolomitic wackestones and packstones with phosphoritic layers (Fig. 5C) that can contain AHC assemblage microfossils. This unit is observed at Jijiapo, Jiuqunao, Hezi'ao, and Wangzishi sections (Appendix 2-5). Fossiliferous peloids are common (up to 400 μm), and the unit is organic-rich, with some microbored grains (Fig. 5B) and sparse silicified lithoclasts. Beds are typically structureless, though roughly planar bedding is infrequently observed.

The third unit is defined by 1.1 to 5 m of phosphoritic silicified phosphatic lime wackestones and packstones containing microfossils (Fig. 5D, 5E). Peloids range typically between 40 and 200 μm in size. This facies forms the basal unit at Baiguotang and is observed at Jijiapo, Jiuqunao, and Hezi'ao (Appendix 1-5).

The fourth unit ranges in thickness between 15 and 38 m in the upper Yanjiahe Formation, as observed in outcrop. It is characterized by a variably thick assemblage of thinly interbedded black shales and lime mudstones and wackestones. This facies always occurs above the first occurrences of acritarchs and SSF. It is primarily observed at Hezi'ao, and is recorded at Jijiapo and Jiuqunao by Jiang et al. (2012).

Unit five measures 13-17 m thick and is defined by the occurrence of coarse recrystallized limestone. Sparse skeletal fragments (phosphatic SSFs, *Chancelloria*-like sclerites), lingulid brachiopods, and fossilized embryos are found. This facies occurs at Hezi'ao and Wangzishi sections (Appendix 4-5).

Liuchapo Formation

The Liuchapo Formation comprises successions of silicified black organic-rich to silty shales and thin silicified dolomitic mudstones, with a total thickness of about 5-9 m on the outer shelf (Ganziping and Daping) that increases basinward to a maximum thickness of 65 m at Longbizui (Fig. 4). All facies observed in the Liuchapo Formation contain small to moderate amounts of anhedral dolomite crystals (< 5%). Phosphatic grains are less common in basinal sections (Longbizui, Louyixi, Jianxincun), but more frequent on the slope transition (Daping, Taoying, Siduping, Xugongping).

Facies one (0.2-10 m) forms the basal unit of the Liuchapo Formation and is a peloidal packed shale that contains abundant disarticulated *H. minor* and *P. jiumenensis*. It typically occurs near the base of the Liuchapo Formation between Daping on the outermost shelf rim and Jianxincun in the deep basin (Appendix 8-15). Peloids are commonly less than 200 μm. At

Ganziping, micritic lithoclasts bearing disarticulated sponge spicules can also be observed (Fig. 6A).

Facies two is 0.2 – 7 m thick, represented by planar bedded to laminated organic-rich black shales (Fig. 6B). This facies typically occurs in the basinal sections between Siduping and Louyixi (Appendix 10-12), and less frequently at Jianxincun (Appendix 15). Strata at Louyixi are dominated by siliceous organic-rich shales.

In facies three (0.5 – 3 m thick), there are convoluted laminae and massively layered shales with lithoclasts (Fig. 6C) and disarticulated microfossils (Fig. 6D) commonly observed in localities at Ganziping, Siduping, and Xugongping (Appendix 6, 10, 11). Soft-sediment deformation structures at Ganziping are observed at decimeter scale (Fig. 6E). Thin sections from Daping, Siduping, and Xugongping exhibit massive to convoluted lamination, frequently occurring with disarticulated bioclasts and rare peloids.

Facies four comprises 0.2 – 2 m of silty shales and dolomitic mudstones that commonly occur at or near the top of the Liuchapo formation at Ganziping, Daping, and Longbizui (Appendix 6, 8, 13). Angular quartz silt grains are common, as are parallel-oriented clay minerals (typically illite). Silicified microcrystalline lithoclasts are rare, but occur in several strata between Ganziping and Daping.

Facies five (0.8 – 6 m) is dominated by silicified phosphatic wackestones and packstones (Fig. 6F). This facies occurs at the top of Longbizui, Yanwutan, and Jianxincun (Appendix 13-15), and contains sparse to abundant AHC assemblage fossils. Peloids range in size from 100-400 μm and are common to abundant in each section.

Niutitang Formation

The basal unit of the Niutitang Formation has been sampled at Sancha, Longbizui, and Taoying. This unit comprises a succession of organic-rich black shale with a basal siliceous phosphoritic bed. At all three localities, the Niutitang exhibits bioclastic thin lenses rich in sponge spicules.

The lowermost portion of the Niutitang at Sancha is characterized by peloidal phosphatic shales exhibiting planar lamination to massive bedding, with outsized chert lithoclasts rarely observed. The basal silicified phosphoritic unit is recognized in thin section as an organic-rich peloidal, spicular shale that contains AHC assemblage microfossils at both Sancha and Longbizui. The metalliferous ore layer was also observed in the Niutitang from outcrops at Sancha, Daping, and from Taoying.

Biostratigraphy

The stratigraphic distributions of Ediacaran macrofossils and Cambrian microfossils are presented in Appendix 1-15. Microfossils of the AHC assemblage zone occur in the Yanjiahe Formation, basal Niutitang phosphorite, and upper Liuchapo Formation. The Ediacaran fossils of the HmPj assemblage occur exclusively in the Liuchapo Formation, with no representatives in the Yanjiahe or Niutitang formations. In all 11 localities in which both assemblages are observed, the first occurrence of the AHC assemblage postdates the last occurrence of the HmPj assemblage. With the exception of the Baiguotang section, the innermost shelf locality observed, AHC assemblage microfossils occur before the first occurrence of any SSF assemblage fossils.

HmPj Assemblage Zone

P. jiumenensis is frequently observed as disarticulated meniscate plates (Fig. 7A), though it is more commonly articulated than *H. minor*. It exhibits a smaller size range (0.1-0.5 mm width), than other palaeopascichnid species (e.g., *P. delicatus*), and is commonly observed inside quartz-pure haloes. Plate concavity (length to depth ratio) ranges between 1.2 and 4.0. It is typically less abundant than *H. minor*, with few isolated exceptions, and strings are seen in close proximity each other in thin sections, but never crossing.

Horodyskia minor is observed at Ganziping, Daping, and most slope and basin outcrop sections (Appendix 6, 8-13, 15). Specimens observed from thin sections consist of beads ranging in size from 0.1 to 1 mm in maximum diameter. Length varies with degree of disarticulation, but beads are typically flattened along bedding planes (~ 1.5 to 2.7:1 L:W ratio). Spheroids are typically separated within a quartz-rich halo, but contact between beads is rarely observed, especially among disarticulated specimens (Fig.7B). Specimens do not typically cross bedding planes. In fact, most specimens are disarticulated spheroids that are randomly oriented within bedding planes, and in some instances, comprise thin bioclastic laminae. Some exceptionally preserved specimens have quartz-pure haloes surrounding the string of beads. Specimens are infrequently observed pressed against each other, but never crossing each other.

All specimens of both *H. minor* and *P. jiumenensis* are silicified. Some occurrences of discs and meniscate plates contain pyrite crystals, and still others contain sub-parallel-oriented platy clay minerals (illite). The HmPj assemblage is dominated by *P. jiumenensis* and *H. minor*, with infrequent occurrences of large, smooth-walled acritarchs of the genus *Leiosphaeridia* (Fig. 7C).

AHC Assemblage Zone

In most cases, AHC microfossils occur in high abundance within a single thin section, with vesicle walls and processes intact and undamaged. Many acritarchs are observed in clumps, though some can be found individually. Some are observed within silicified mudstones, but AHC acritarchs are most typically found in siliceous and phosphatic peloidal wackestones and packstones, frequently in peloids. Species diversity is low, comprising up to 5 acritarch taxa, with 3-6 co-occurring SSFs, tubular microfossils, and non-diagnostic morphotypes, including *Leiosphaeridia* sp. (Fig. 7D) and the cyanobacterium *Siphonophycus robustum*. However, diversity is much higher within the AHC assemblage zone than in the HmPj assemblage zone.

Among the acanthomorphic acritarchs specifically used to identify the AHC horizon, *Heliosphaeridium ampliatum* (formerly *Micrhystridium ampliatum*) is the most abundant (Fig. 8A-C), in some instances reaching population densities of several hundred per cm^2 in thin sections. *H. ampliatum* is observed across the entire inner carbonate shelf, and occurs in the lower Niutitang phosphorite at Sancha and Taoying, as well as in the uppermost Liuchapo Formation at Xugongping, Longbizui, Louyixi, Yanwutan, and Jianxincun in the slope and basin. In observed sections, *H. ampliatum* vesicles range in diameter from 3.4 to 10.8 μm, with hollow, distally-tapering processes ranging in length from 5.0 to 15.6 μm. Up to 12 processes are present in a circumferential view. Modeled surface area to volume ratios of individuals ranges between 1.2 and 1.6 μm^{-1}, with spine to body length ratios of 0.7 to 1.9. This species is frequently observed in clumps and in rounded organic-rich peloids, many of which have broken processes, or are stripped of processes, with varying degrees of damage to vesicle walls. Specimens observed outside of these peloids are solitary, and are usually undamaged.

Comasphaeridium annulare is the second most abundant acritarch observed (Fig. 8D-E). It is observed to have smaller vesicle sizes (3.9 – 7.9 μm), and shorter, though more abundant, hollow processes (0.9 – 1.6 μm in length, up to 28 processes in circumferential view), than those observed in *H. ampliatum*. The densely packed processes sometimes have organic matter or pyrite on or near their tips. The modeled surface area to volume ratio ranges between 0.8 and 1.61 μm^{-1}, with spine to body length ratio between 0.17 and 0.22. *C. annulare* is never observed in close aggregation with other acritarchs, commonly observed individually in the matrix of peloidal wackestones and packstones, though, like *Heliosphaeridium*, it can be present inside peloids with significant degradation of processes. *C. annulare* also has basin wide distribution in the Yanjiahe Formation and the uppermost Liuchapo Formation at Taoying (also in Niutitang), Xugongping, Longbizui, Louyixi, Yanwutan, and Jianxincun.

Less frequently observed in thin section are the tubular fossil *Megathrix longus* and the acanthomorph *Asteridium tornatum* (Fig. 8F). *M. longus* varies in its occurrence, appearing as individual tubes or tubular aggregates. Internal structure is marked by a characteristic corrugated transverse cross-wall (Fig. 8G). Specimen width is typically 90-100 μm. *A. tornatum* is an acanthomorphic acritarch that is only observed as solitary specimens and, like *H. ampliatum*, it can be observed in close association with organic-rich peloids. *A. tornatum* has an observed size range of 5.5 to 8.2 μm with process lengths ranging between 1.5 and 2.4 μm and arranged sparsely on vesicle wall (up to 16 processes in circumferential view). Modeled surface area to volume ratio is 0.78 to 0.85 μm^{-1}, with a spine to body length ratio of 0.21 to 0.31. *A. tornatum* is observed in the Yanjiahe Formation at Jiuqunao and Hezi'ao, the uppermost Liuchapo Formation at Longbizui and Jianxincun, and the basal Niutitang phosphorite bed at Sancha.

Skeletal Fragments (SSF and Sponge Spicules)

Small shelly fossils commonly occur alongside AHC acritarchs, but are comparatively rare in most sections. *Kaiyangites novilis* is the most frequently observed SSF across localities (Fig. 9A-B), occurring in the Yanjiahe Formation at Baiguotang, Jiuqunao, and Hezi'ao. *K. novilis* specimens exhibit an arcuate shape in thin section that reflects their rounded, conical shape. Size dimensions range in length between 167 and 455 μm, with a concavity depth of 87 to 327 μm, and shell thickness ranging between 6.0 and 48 μm. Also reported, from the upper 9 m of the Yanjiahe Formation at Wangzishi, abundant brachiopods, including acrotretid and obolellid brachiopods can be found. Abundant *Chancelloria*-like sclerites are also observed in the upper 12 m in the same section, as are calcitized putative animal embryo fossils (uppermost 11 m). Sponge spicules are also present within these strata as calcitized casts. SSFs exhibit variable preservation quality, as they occur within recrystallized limestone that dominates the upper Yanjiahe at Wangzishi. *Anabarites trisulcatus* has been identified from Yanjiahe float at Jijiapo (Fig. 9C) and a triangular tubular SFF has been observed in situ from Yanjiahe phosphoritic chert at Baiguotang (Fig. 9F).

Sponge spicules occur within Cambrian strata alongside AHC assemblage fossils (Fig. 9D-E, 9G). All observed spicules probably belong to the Class Hexactinellida (glass sponges). Spicules are typically monactine or diactine, with less abundant hexactine spicules, occurring in the Yanjiahe Formation at Baiguotang, Jijiapo, Jiuqunao, and Hezi'ao (Appendix 1-4), in siliceous sediments of the Liuchapo at Siduping, Xugongping, Louyixi, Longbizui, Yanwutan, and Jianxincun, and in shales of the Niutitang Formation at Ganziping, Sancha, Taoying, Siduping, and Longbizui. Spicules are typically preserved as casts. In some cases, a black

organic coating is preserved (Fig. 6F, 9G), possibly representing the axial filament of sponge spicules. In the Niutitang Formation at Siduping, pyritized sponge body fossils and spicules up to several centimeters in length are observed in shale slabs. Spicules in thin section are 3.2 to 107 μm in diameter and up to ~1.7 mm in length.

Non-diagnostic Fossils

Nondiagnostic fossils include the cyanobacterium *Siphonophycus robustum*, triad and tetrad *Archaeophycus yunnanensis*, and the smooth-walled *Leiosphaeridia* (Eisenack, 1958) (Fig. 7C, 7D). *Leiosphaeridia* is by far the most common. Vesicles are collapsed, and vesicle walls are thick (0.9 – 1.5 μm). Vesicle diameters estimated from the perimeters of collapsed specimens are 1.5 mm and 1.7 mm for individuals co-occurring with Ediacaran and Cambrian fossils, respectively. These fossils are less abundant in strata associated with Ediacaran fossils, and much more abundant (up to dozens per thin section) in Cambrian strata. *Leiosphaeridia* is more frequent in mudstones than AHC microfossils, though like AHC microfossils, they are more abundant in peloidal packstones. Some *Leiosphaeridia* are broken, but most have intact vesicle walls. Being so large and without surface ornamentation, their surface area to volume ratio is estimated between 0.004 and 0.027 μm^{-1}.

Fossil Assemblages and the Carbon Isotopic Record

When compared to the carbon isotope record of the Yanjiahe Formation (Figure 10A-C) (Jiang et al., 2012), AHC acritarchs at Jijiapo and Jiuqunao first occur alongside a large negative isotope excursion in the lower Yanjiahe Formation. AHC acritarchs appear to reach their peak abundance within 1-2 m after their first occurrence, a pattern that aligns with the negative carbon

isotope excursion. Ishikawa et al. (*in press*) also note the negative excursion within the Yanjiahe Formation from drill core in the Yangtze Gorges area (from 0‰ at the base, decreasing to -7‰ approximately 13 m above the base) that coincides with increasing acritarch abundance and diversification. The lack of *Micrhystridium*-like acritarchs at observed basal strata in the present study does not support acritarch origination coinciding with the base of the Yanjiahe Formation. Instead, the occurrence of AHC acritarchs approximately 11 to 16 m above the base of the formation (Appendix 2-5), indicates that Yanjiahe Formation deposition may have occurred prior to the deposition or preservation of Cambrian forms. The first occurrence of AHC acritarchs consistently occurs within the negative carbon isotope excursion, typically near the most negative values.

A similar agreement of data occurs between the first occurrences of AHC within the Liuchapo Formation at Longbizui, Hunan Province, South China (Fig. 11). Though inorganic carbon is not available for the Liuchapo Formation, organic carbon isotope data have been published (Wang et al., 2012a), suggesting the Ediacaran-Cambrian boundary at approximately 40 m above the base of the Liuchapo based on a negative organic carbon isotope shift (–34.6 to –7.3 ‰). In the current study, the first occurrence of AHC acritarchs directly coincides with the negative isotope excursion (Fig. 11).

Discussion

In light of issues surrounding the reliability of the current position of the GSSP at Fortune Head, Newfoundland, there is need to reconsider the official definition of the Ediacaran-Cambrian boundary. Gehling et al. (2001) suggest leaving the GSSP in place, as it marks first occurrence of diverse, abundant, complex trace fossils that likely reflect major behavioral change among

metazoans. However, such a solution does not address the larger problems associated with facies dependence of *T. pedum* and with its limited global correlation potential. The same is true for the prospect of moving the GSSP to the new FAD of *T. pedum*.

The prospect of using SSF should be taken with caution, as many SSF occurrences of late Ediacaran and earliest Cambrian are strongly facies dependent, occurring in mainly phosphatic carbonates. Currently recognized assemblages are of demonstrably regional importance, but their global occurrence remains to be shown. The negative carbon isotope anomaly itself could be used to define Cambrian strata and a new GSSP selected, but the carbon isotope anomaly cannot be correlated to siliciclastic strata. Furthermore, given that facies-related $\delta^{13}C$ variations are superimposed on secular variations, it is difficult to precisely define a point in $\delta^{13}C$ excursions for global correlation.

Conversely, AHC microfossils display desirable qualities of index fossil candidates. They occur within lime mudstones, wackestones, packstones, and shales deposited within a variety of environments along a shelf to basin transect. Though they are taphonomically dependent, occurring only in silicified sediments, they are environmentally independent. Morphological characters, including vesicle diameter and ornamentation, are readily observable quantities for ease of species identification. AHC assemblage fossils also consistently overlie the last occurrences of HmPj assemblage fossils, displaying no overlap with previously established Ediacaran fossils. Though the lack of HmPj fossils in the lowermost Yanjiahe may be facies controlled, AHC microfossils display very little facies control, occurring in silicified mudstones, wackestones, packstones, and siliceous shales. The fact that both assemblages occur in silicified strata supports the interpretation that the lack of overlap observed between the two assemblages is real. AHC acritarchs have proven useful in correlation at regional- (Yao et al., 2005) and

global-scale (Moczydlowska, 2011; Yao et al., 2005). Furthermore, the constrained stratigraphic distribution of HmPj and AHC assemblages, specific to Ediacaran and Lower Cambrian strata worldwide, respectively, supports the use of these assemblages to bracket the Ediacaran-Cambrian boundary.

These assemblages also occur in chert-carbonate successions at Jijiapo, Jiuqunao, Hezi'ao, Longbizui, and Yanwutan, where carbon isotopic data are available, making it possible to calibrate the AHC-based biostratigraphy with carbon isotope chemostratigraphy (Jiang et al., 2012). Both the $\delta^{13}C_{carb}$ (Jijiapo, Jiuqunao, Hezi'ao) and $\delta^{13}C_{org}$ (Longbizui) display negative isotope excursions that are used to identify the Ediacaran-Cambrian boundary. The consistent alignment of the FAD of AHC acritarchs with the negative $\delta^{13}C$ anomalies demonstrates that redefining the Cambrian GSSP with an AHC candidate will not significantly displace the base of the Cambrian System from its current chronostratigraphic position.

Conclusions

Recent discoveries have raised significant questions about the reliability of using the trace fossil *T. pedum* to define the base of the Cambrian System, including facies dependence, poor resolution on morphology and preservation, and its discovery several meters below the GSSP at Fountain Head, Newfoundland. Defining a new GSSP, based on a new index fossil, is necessary, as the current definition is undermined by the presence of complex burrow structures below the current GSSP and by the facies dependence of *T. pedum*, limiting its correlation potential to carbonate successions, where SSF and carbon isotope data is most useful. It is proposed that acanthomorphic acritarchs of the AHC assemblage be considered for defining the base of the Cambrian System. Facies independence, cosmopolitan distribution across carbonate and fine-

grained siliciclastic successions, and short stratigraphic range establish the AHC assemblage as a useful biostratigraphic tool to redefine the base of the Cambrian System.

Of the AHC acanthomorphs, *Heliosphaeridium ampliatum* exhibits the widest areal distribution and greatest abundance. *H. ampliatum* is easily distinguishable from other AHC acritarchs by their long and rigid processes. It is also temporally restricted to Cambrian Stage 1 and Stage 2 (Terreneuvian) strata (Wang, 1985; Yao et al., 2005). In order to ensure precise definition of the base of the Cambrian System, the FAD of *H. ampliatum* from the AHC assemblage is proposed to define the new Cambrian GSSP in South China.

Works Cited

Buatois, L. A., Almond, J., and Germs, G. J. B., 2013, Environmental tolerance and range offset of *Treptichnus pedum*: Implications for the recognition of the Ediacaran-Cambrian boundary: Geology, v. 41, p. 519–522.

Chen, D., Wang, J., Qing, H., Yan, D., and Li, R., 2009, Hydrothermal venting activities in the Early Cambrian, South China: Petrological, geochronological and stable isotopic constraints: Chemical Geology, v. 258, p. 168-181.

Compston, W., Williams, I. S., Kirschvink, J. L., Zhang Zichao, and Ma Guogan, 1992, Zircon U-Pb ages for the Early Cambrian time-scale: Journal of the Geological Society, London, v. 149, p. 171-184.

Condon, D., Zhu, M., Bowring, S., Wang, W., Yang, A., and Jin, Y., 2005, U-Pb ages from the Neoproterozoic Doushantuo Formation, China: Science, v. 308, p. 95-98.

Corsetti, F. A., and Hagadorn, J. W., 2000, Precambrian-Cambrian transition: Death Valley, United States: Geology, v. 28, p. 299–302.

Ding, L., Li, Y., and Chen, H., 1992, Discovery of *Micrhystridium regulare* from Sinian–Cambrian boundary strata in Yichang, Hubei, and its stratigraphic significance: Acta Micropalaeontologica Sinica, v. 9, p. 303-309.

Dong, L., Song, W., Xiao, S., Yuan, X., Chen, Z., and Zhou, C., 2012, Micro- and macrofossils from the Piyuancun Formation and their implications for the Ediacaran-Cambrian boundary in southern Anhui: Journal of Stratigraphy, v. 36, no. 11, p. 600.

Dong, L., Xiao, S., Shen, B., and Zhou, C., 2008, Silicified *Horodyskia* and *Palaeopascichnus* from upper Ediacaran cherts in South China: tentative phylogenetic interpretation and implications for evolutionary stasis: Journal of the Geological Society of London, v. 165, p. 367-378.

Dong, L., Xiao, S., Shen, B., Zhou, C., Li, G., and Yao, J., 2009, Basal Cambrian microfossils from the Yangtze Gorges area (South China) and the Aksu area (Tarim Block, northwestern China): Journal of Paleontology, v. 83, p. 30-44.

Dunham, R. J., 1962, Classification of carbonate rocks according to depositional texture: American Association of Petroleum Geologists Memoir, v. 1, p. 108-121.

Eisenack, A., 1958, *Tasmanites* Newton 1875 und Leiosphaeridia n. gen. aus Gattungen der Hystrichosphaeridea: Palaeontographica Abteilung A, v. 110, p. 1-19.

Fedonkin, M. A., and Yochelson, E. L., 2002, Middle Proterozoic (1.5 Ga) *Horodyskia moniliformis* Yochelson and Fedonkin, the oldest known tissue-grade colonial eucaryote: Smithsonian Contributions to Paleobiology, v. 94, p. 1-29.

Gehling, J. G., Jensen, S., Droser, M. L., Myrow, P. M., and Narbonne, G. M., 2001, Burrowing below the basal Cambrian GSSP, Fortune Head, Newfoundland: Geological Magazine, v. 138, no. 2, p. 213-218.

Gehling, J. G., Narbonne, G. M., and Anderson, M. M., 2000, The first named Ediacaran body fossil, *Aspidella terranovica*: Palaeontology, v. 43, no. 3, p. 427-456.

Geyer, G., 2005, The Fish River Subgroup in Namibia: stratigraphy, depositional environments and the Proterozoic-Cambrian boundary problem revisited: Geological Magazine, v. 142, p. 465-498.

Grey, K., and Williams, I. R., 1990, Problematic bedding-plane markings from the Middle Proterozoic Manganese Subgroup, Bangemall Basin, Western Australia: Precambrian Research, v. 46(4), p. 307-328.

Guo, J., Li, Y., and Li, G., *in press*, Small shelly fossils from the early Cambrian Yanjiahe Formation, Yichang, Hubei, China: Gondwana Research.

Guo, Q., Strauss, H., Liu, C., Goldberg, T., Zhu, M., Pi, D., Heubeck, C., Vernhet, E., Yang, X., and Fu, P., 2007, Carbon isotopic evolution of the terminal Neoproterozoic and early Cambrian: Evidence from the Yangtze Platform, South China: Palaeogeography Palaeoclimatology Palaeoecology, v. 254, p. 140–157.

Horodyski, R. J., 1982, Problematic bedding-plane markings from the middle Proterozoic Appekunny argillite, Belt Supergroup, northwestern Montana: Journal of Paleontology, v. 56, p. 882-889.
Huntley, J. W., Xiao, S., and Kowalewski, M., 2006, 1.3 billion years of acritarch history: An empirical morphospace approach: Precambrian Research, v. 144, p. 52-68.
Ishikawa, T., Ueno, Y., Komiya, T., Sawaki, Y., Han, J., Shu, D., Li, Y., Maruyama, S., and Yoshida, N., 2008, Carbon isotope chemostratigraphy of a Precambrian/Cambrian boundary section in the Three Gorge area, South China: Prominent global-scale isotope excursions just before the Cambrian Explosion: Gondwana Research, v. 14, p. 193–208.
Ishikawa, T., Ueno, Y., Shu, D., Li, Y., Han, J., Guo, J., Yoshida, N., Maruyama, S., and Komiya, T., *in press*, The δ13C excursions spanning the Cambrian explosion to the Canglangpuian mass extinction in the Three Gorges area, South China: Gondwana Research.
Javaux, E. J., Marshall, C. P., and Bekker, A., 2010, Organic-walled microfossils in 3.2-billion-year-old shallow-marine siliciclastic deposits: Nature, v. 463, p. 934-938.
Jenkins, R. J. F., 1995, The problems and potential of using animal fossils and trace fossils in terminal Proterozoic biostratigraphy: Precambrian Research, v. 73, no. 1-4, p. 51-69.
Jensen, S., 2003, The Proterozoic and earliest Cambrian trace fossil record: patterns, problems and perspectives: Integrative and Comparative Biology, v. 43, p. 219-228.
Jensen, S., Saylor, B. Z., Gehling, J. G., and Germs, G. J. B., 2000, Complex trace fossils from the terminal Proterozoic of Namibia: Geology, v. 28, no. 2, p. 143-146.
Jiang, G., Shi, X., Zhang, S., Wang, Y., and Xiao, S., 2011, Stratigraphy and paleogeography of the Ediacaran Doushantuo Formation (ca. 635-551 Ma) in South China: Gondwana Research, v. 19, p. 831–849.
Jiang, G., Wang, X., Shi, X., and Xiao, S., 2012, The origin of decoupled carbonate and organic carbon isotope signatures in the early Cambrian (ca. 542-520 Ma) Yangtze platform: Earth and Planetary Science Letters, v. 317-318, p. 96-110.
Jiang, S.-Y., Pi, D.-H., Heubeck, C., Frimmel, H., Liu, Y.-P., Deng, H.-L., Ling, H.-F., and Yang, J.-H., 2009, Early Cambrian ocean anoxia in South China: Nature, v. 459, p. E5-E6.
Jiang, S. Y., Yang, J. H., Ling, H. F., Chen, Y. Q., Feng, H. Z., Zhao, K. D., and Ni, P., 2007, Extreme enrichment of polymetallic Ni-Mo-PGE-Au in Lower Cambrian black shales of South China: An Os isotope and PGE geochemical investigation: Palaeogeogr Palaeoclimatol Palaeoecol, v. 254, no. 1-2, p. 12-12.
Khomentovskii, V. V., and Karlova, G. A., 2005, The Tommotian Stage base as the Cambrian lower boundary in Siberia: Stratigraphy and Geological Correlation, v. 13, p. 21-34.
Knoll, A. H., 1994, Proterozoic and Early Cambrian protists: Evidence for accelerating evolutionary tempo: Proceedings of the National Academy of Sciences, USA, v. 91, p. 6743-6750.
Knoll, A. H., Kaufman, A. J., Semikhatov, M. A., Grotzinger, J. P., and Adams, W., 1995, Sizing up the sub-Tommotian unconformity in Siberia: Geology, v. 23, no. 12, p. 1139-1143.
Landing, E., 1994, Precambrian-Cambrian boundary global stratotype ratified and a new perspective of Cambrian time: Geology, v. 22, p. 179-182.
Li, G., and Holmer, L. E., 2004, Early Cambrian lingulate brachiopods from the Shaanxi Province, China: GFF, v. 126, no. 2, p. 193-211.
Li, G., Steiner, M., Zhu, M., and Zhao, X., 2012, Early Cambrian eodiscoid trilobite *Hupeidiscus orientalis* from South China: Ontogeny and implications for affinities of *Mongolitubulus*-like sclerites: Bulletin of Geosciences, v. 87, no. 1, p. 11.
Li, G., Zhu, M., Steiner, M., and Qian, Y., 2004, Skeletal faunas from the Qiongzhusian of southern Shaanxi: Biodiversity and lithofacies-biofacies lilnks in the Lower Cambrian carbonate settings: Progress in Natural Science, v. 14, no. 1, p. 6.

Li, Z. X., Bogdanova, S. V., Collins, A. S., Davidson, A., Waele, B. D., Ernst, R. E., Fitzsimons, I. C. W., Fuck, R. A., Gladkochub, D. P., Jacobs, J., Karlstrom, K. E., Lu, S., Natapov, L. M., Pease, V., Pisarevsky, S. A., Thrane, K., and Vernikovsky, V., 2008, Assembly, configuration, and break-up history of Rodinia: A synthesis: Precambrian Research, v. 160, p. 179–210.

Maloof, A. C., Porter, S. M., Moore, J. L., Dudás, F. Ö., Bowring, S. A., Higgins, J. A., Fike, D. A., and Eddy, M. P., 2010, The earliest Cambrian record of animals and ocean geochemical change: Geological Society of America Bulletin, v. 122, p. 1731–1774.

Mathur, V. K., and Srivastava, D. K., 2004, Record of tissue grade colonial eucaryote and microbial mat associated with Ediacaran fossils in Krol group, Garhwal syncline, Lesser Himalaya, Uttaranchal: Journal of the Geological Society of india, v. 63, p. 100-102.

McFadden, K. A., Xiao, S., Zhou, C., and Kowalewski, M., 2009, Quantitative evaluation of the biostratigraphic distribution of acanthomorphic acritarchs in the Ediacaran Doushantuo Formation in the Yangtze Gorges area, South China: Precambrian Research, v. 173, p. 170-190.

Moczydlowska, M., 2011, The early Cambrian phytoplankton radiation: Acritarch evidence from the Lukati Formation of Estonia: Palynology, v. 35, no. 1, p. 43.

Moczydłowska, M., 1991, Acritarch biostratigraphy of the Lower Cambrian and the Precambrian–Cambrian boundary in southeastern Poland: Fossils and Strata, v. 29, p. 1-127.

Montenari, M., and Leppig, U., 2003, The Acritarcha: their classification, morphology and palaeoecological/palaeogeographical distribution: Palaontogische Zeitschrift, v. 67, p. 21.

Narbonne, G. M., Myrow, P. M., Landing, E., and Anderson, M. M., 1987, A candidate stratotype for the Precambrian-Cambrian boundary, Fortune Head, Burin Peninsula, southeastern Newfoundland: Canadian Journal of Earth Sciences, v. 24, p. 1277-1293.

Palij, V. M., 1976, Remains of non-skeletal fauna and trace fossils from upper Precambrian and Lower Cambrian deposits of Podolia, *in* Ryabenko, V. A., ed., Paleontology and Stratigraphy of the upper Precambrian and lower Paleozoic of the south-western part of the East European Platform: Kiev, Naukova Dumka, p. 63-77.

Palij, V. M., Posti, E., and Fedonkin, M. A., 1979, Soft-bodied Metazoa and animal trace fossils in the Vendian and Early Cambrian, *in* Urbanek, A., and Rozanov, A. Y., eds., Upper Precambrian and Cambrian Paleontology of the East-European Platform: Warszawa, Wydawnictwa Geologiczne, p. 56-94 (In Russian, English edition published in 1983).

Peng, S., Babcock, L., and Cooper, R., 2012, The Cambrian period, *in* Gradsteain, F. M., Ogg, J. G., Schmitz, M., and Ogg, G., eds., The Cambrian Time Scale 2012, Elsevier, p. 52.

Peng, S., and Babcock, L. E., 2001, Cambrian of the Hunan-Guizhou region, South China, *in* Peng, S., Babcock, L. E., and Zhu, M., eds., Cambrian System of South China (Palaeoworld No. 13): Hefei, University of Science and Technology of China Press, p. 3-51.

Porter, S. M., 2004, Closing the phosphatization window: Testing for the influence of taphonomic megabias on the pattern of small shelly fossil decline: Palaios, v. 19, p. 178–183.

Qian, Y., Li, G., and Zhu, M., 2001, The Meishucunian Stage and its small shelly fossil sequence in China: Acta Palaeontologica Sinica, v. 40 (supplement), p. 54-62.

Qian, Y., and Yin, G., 1984, Small shelly fossils from the lowest Cambrian in Guizhou: Professional Papers of Stratigraphy and Palaeontology, v. No. 13, p. 91-124.

Seilacher, A., 2007, Trace Fossil Analysis, Berlin, Springer, 226 p.:

Seilacher, A., Grazhdankin, D., and Legouta, A., 2003, Ediacaran biota: The dawn of animal life in the shadow of giant protists: Paleontological Research, v. 7, no. 1, p. 43-54.

Siegmund, H., and Erdtmann, B.-D., 1994, Facies and diagenesis of some Upper Proterozoic dolomites of South China: Facies, v. 31, p. 255-264.

Steiner, M., Li, G., Qian, Y., Zhu, M., and Erdtmann, B.-D., 2007, Neoproterozoic to early Cambrian small shelly fossil assemblages and a revised biostratigraphic correlation of the Yangtze Platform (China): Palaeogeography, Palaeoclimatology, Palaeoecology, v. 254, p. 67-99.

Steiner, M., Wallis, E., Erdtmann, B.-D., Zhao, Y., and Yang, R., 2001, Submarine-hydrothermal exhalative ore layers in black shales from South China and associated fossils -- insights into a Lower Cambrian facies and bio-evolution: Palaeogeography, Palaeoclimatology, Palaeoecology, v. 169, p. 165-191.

Steiner, M., Zhu, M., Zhao, Y., and Erdtmann, B.-D., 2005, Lower Cambrian Burgess Shale-type fossil associations of South China: Palaeogeography Palaeoclimatology Palaeoecology, v. 220, p. 129-152.

Tiwari, M., 1999, Organic-walled microfossils from the Chert-phosphorite Member, Tal Formation, Precambrian--Cambrian boundary, India: Precambrian Research, v. 97, p. 99-113.

Vannier, J., Calandra, I., Gaillard, C., and Żylińska, A., 2010, Priapulid worms: Pioneer horizontal burrowers at the Precambrian-Cambrian boundary: Geology, v. 38, p. 711–714.

Wang, C. S., and Pien, H. T., 1949, Notes on the Pre-Devonian Stratigraphy of the Middle Tzekiang1 Valley, W Hunan*: Bulletin of the Geological Society of China, v. 29, no. 1-4, p. 63-74.

Wang, F., 1985, Middle -- upper Proterozoic and lowest Phanerozoic microfossil assemblage from SW China and contiguous areas: Precambrian Research, v. 29, p. 33-43.

Wang, J., Chen, D., Yan, D., Wei, H., and Xiang, L., 2012a, Evolution from an anoxic to oxic deep ocean during the Ediacaran-Cambrian transition and implications for bioradiation: Chemical Geology, v. 306–307, p. 129-138.

Wang, X., Shi, X., Jiang, G., and Zhang, W., 2012b, New U-Pb age from the basal Niutitang Formation in South China: Implications for diachronous development and condensation of stratigraphic units across the Yangtze platform at the Ediacaran-Cambrian transition: Journal of Asian Earth Sciences, v. 48, p. 8.

Wilson, J. P., Grotzinger, J. P., Fischer, W. W., Hand, K. P., Jensen, S., Knoll, A. H., Abelson, J., Metz, J. M., McLoughlin, N., Cohen, P. A., and Tice, M. M., 2012, Deep-water incised valley deposits at the Proterozoic-Cambrian boundary in southern Namibia contain abundant *Treptichnus pedum*: Palaios, v. 27, p. 252–273.

Yao, J., Xiao, S., Yin, L., Li, G., and Yuan, X., 2005, Basal Cambrian microfossils from the Yurtus and Xishanblaq formations (Tarim, north-west China): Systematic revision and biostratigraphic correlation of *Micrhystridium*-like acritarchs from China: Palaeontology, v. 48, p. 687-708.

Yochelson, E. L., and Fedonkin, M. A., 2000, A new tissue-grade organism 1.5 billion years old from Montana: Proceedings of the Biological Society of Washington, v. 113, no. 3, p. 843-847.

Zhang, X., Liu, W., and Zhao, Y., 2008, Cambrian Burgess Shale-type Lagerstätten in South China: Distribution and significance: Gondwana Research, v. 14, no. 1–2, p. 255-262.

Zhang, X., Shu, D., Li, Y., and Han, J., 2001, New sites of Chengjiang fossils; crucial windows on the Cambrian explosion: Journal of the Geological Society of London, v. 158, no. 2, p. 211-218.

Zhao, G., and Cawood, P. A., 2012, Precambrian geology of China: Precambrian Research, v. 222-223, p. 42.

Zhu, M., Zhang, J., Steiner, M., Yang, A., Li, G., and Erdtmann, B.-D., 2003, Sinian-Cambrian stratigraphic framework for shallow- to deep-water environments of the Yangtze Platform: an integrated approach: Progress in Natural Science, v. 13, p. 951-960.

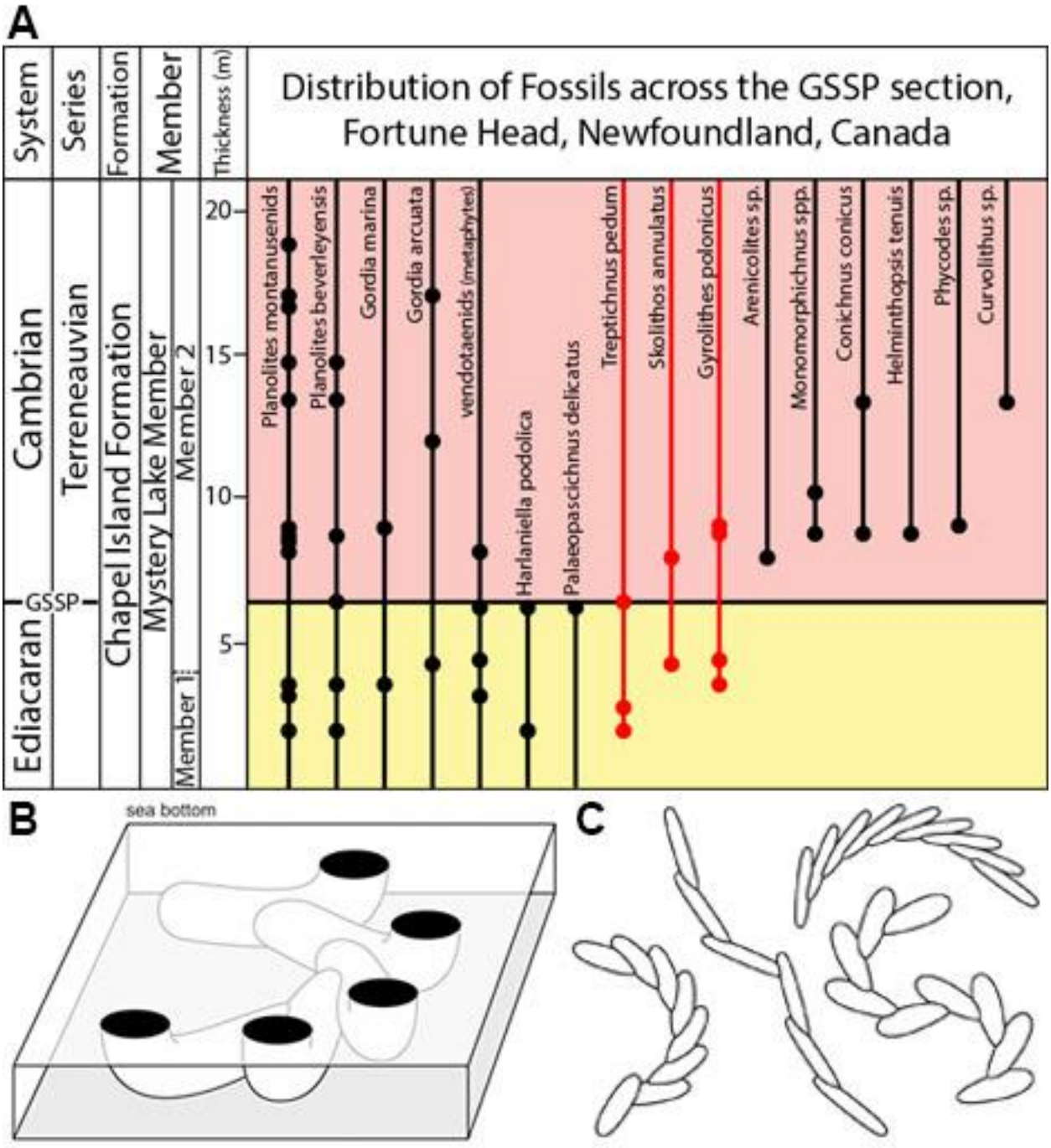

Figure 1. Trace fossil occurrences at the Ediacaran-Cambrian boundary GSSP section at Fortune Head, Newfoundland, Canada. A) Schematic diagram of fossil occurrences across the Cambrian GSSP, from Peng et al. (2012) and Gehling et al. (2001). *Harlaniella podolica* and *Palaeopascichnus delicatus* do not persist above the GSSP. *Treptichnus pedum*, *Skolithos annulatus*, and *Gyrolithes polonicus*, are shown in red. B) Oblique view, schematic diagram of *T. pedum* sub-horizontal burrowing pattern, and C) Plane view, schematic diagram of *T. pedum* burrowing pattern (http://en.wikipedia.org/wiki/Treptichnus_pedum).

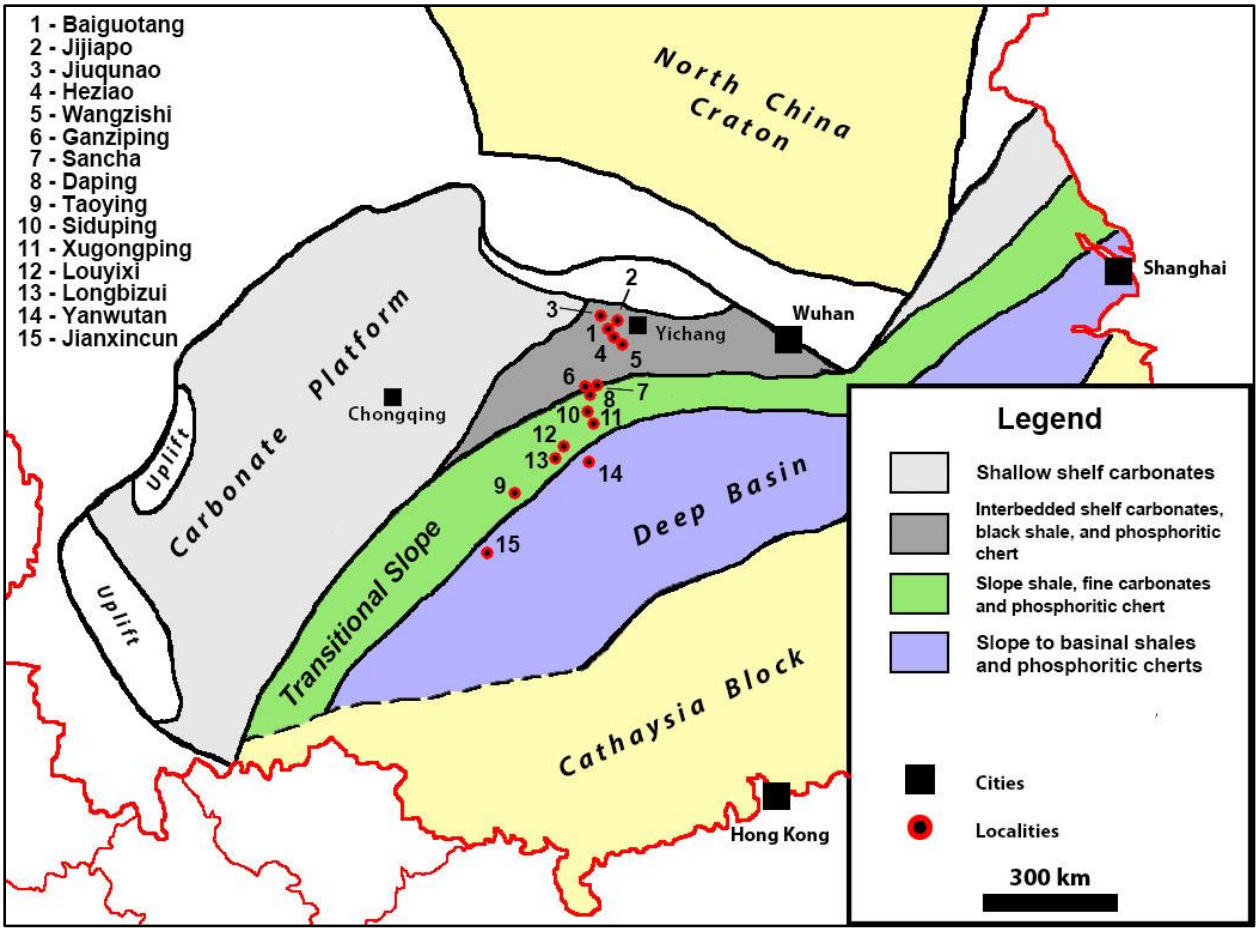

Figure 2. Locality map of South China Block with depositional environment subdivisions. Modified from (Jiang et al., 2007).

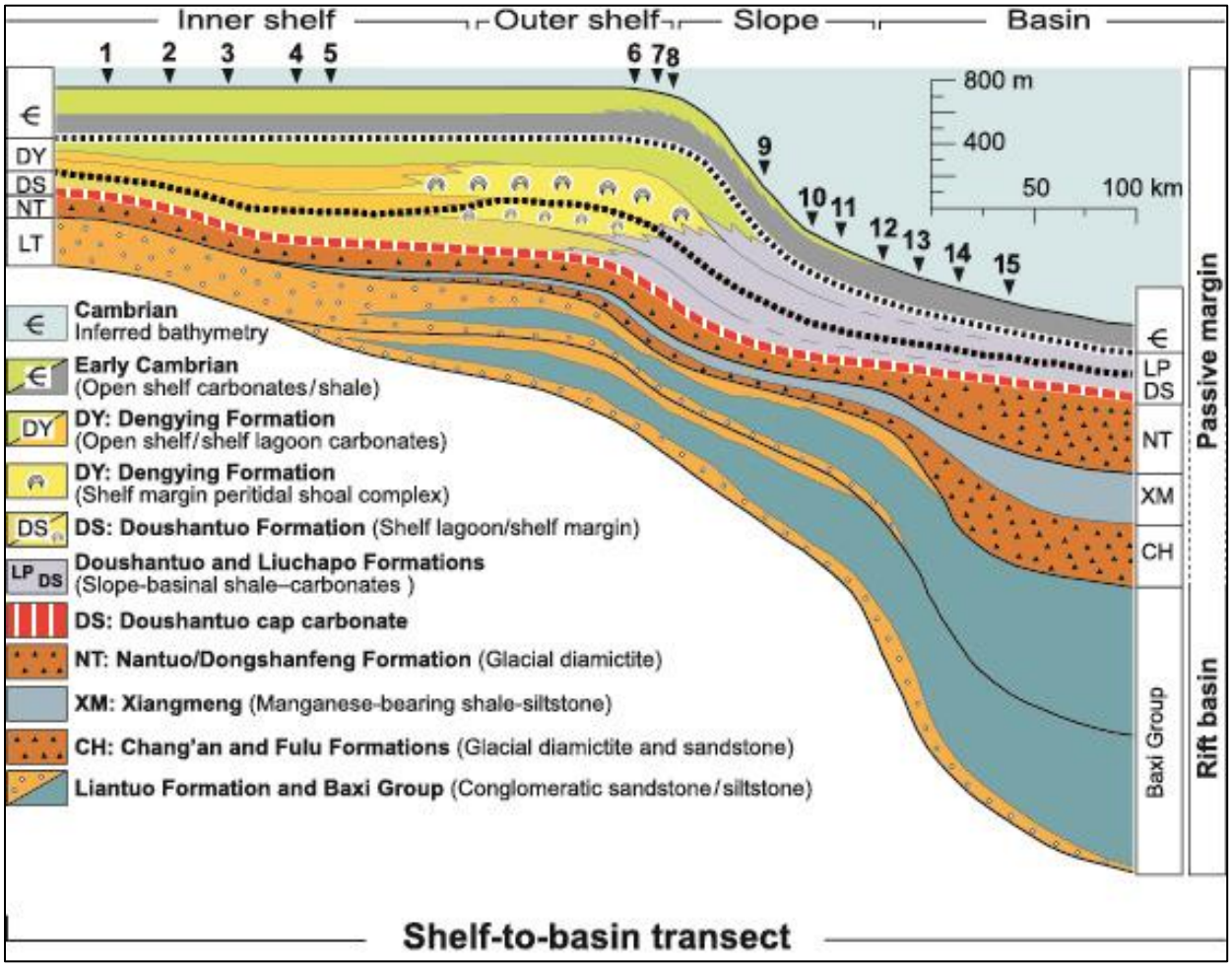

Figure 3. Yangtze carbonate platform to basin cross-section. Numbers correspond to numbered localities in Figures 2 and 4. Positions along cross section indicate position of locality on shelf to platform transect. Modified from Jiang et al. (2012).

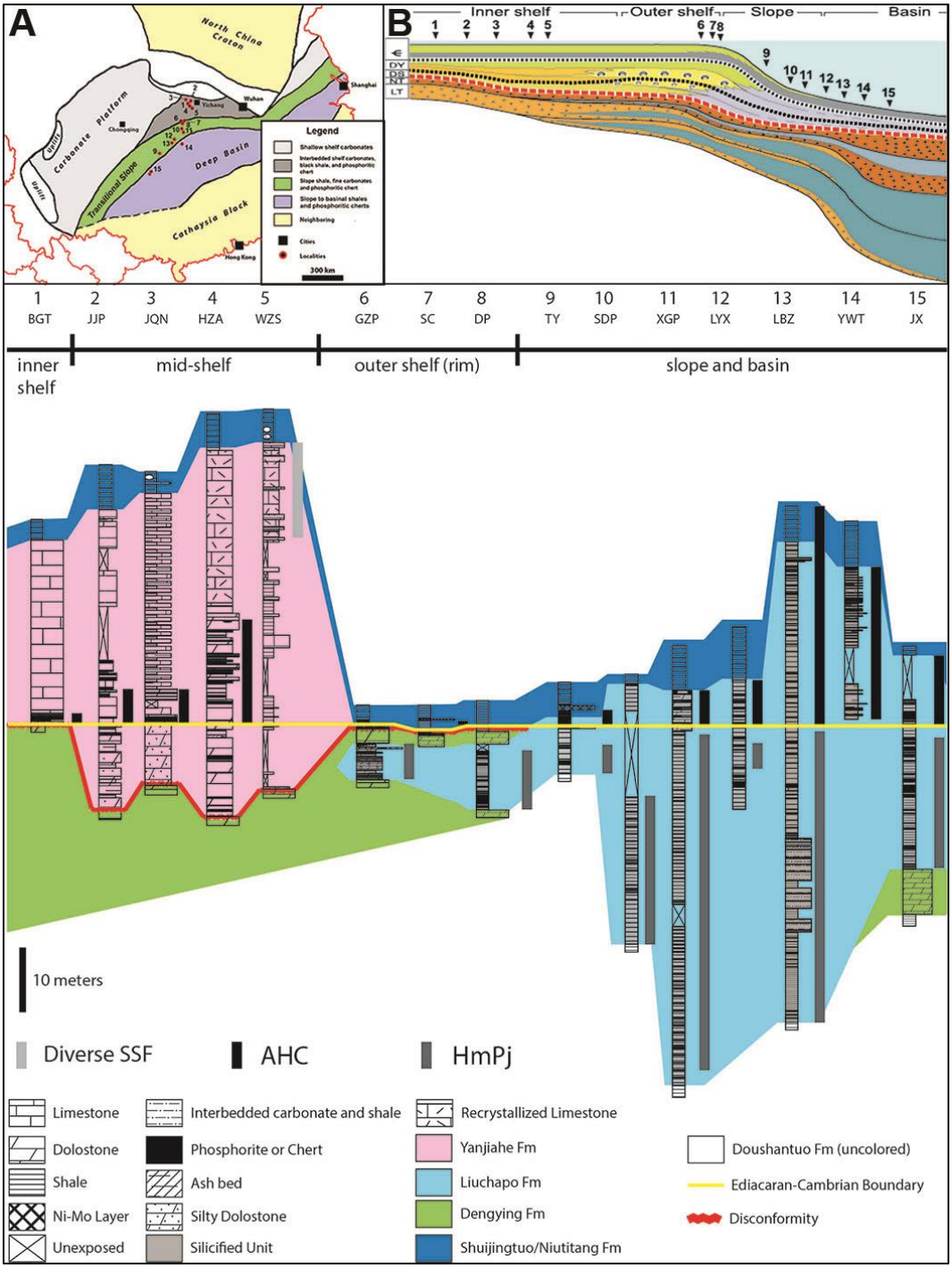

Figure 4. Stratigraphic sections and correlation of studied localities. A) Localities of South China. B) Yangtze Platform cross-section. Bottom) Stratigraphic relationship of Ediacaran (Doushantuo, Dengying, Liuchapo, and Yanjiaheformations) and Cambrian (Yanjiahe, Liuchapo, Shuijingtuo, and Niutitang formations). AHC and HmPj zones are shown next to each column. The red line represents disconformable contacts between Yanjiahe and Dengying formations. The yellow line represents the placement of the Ediacaran-Cambrian boundary based on fossil evidence.

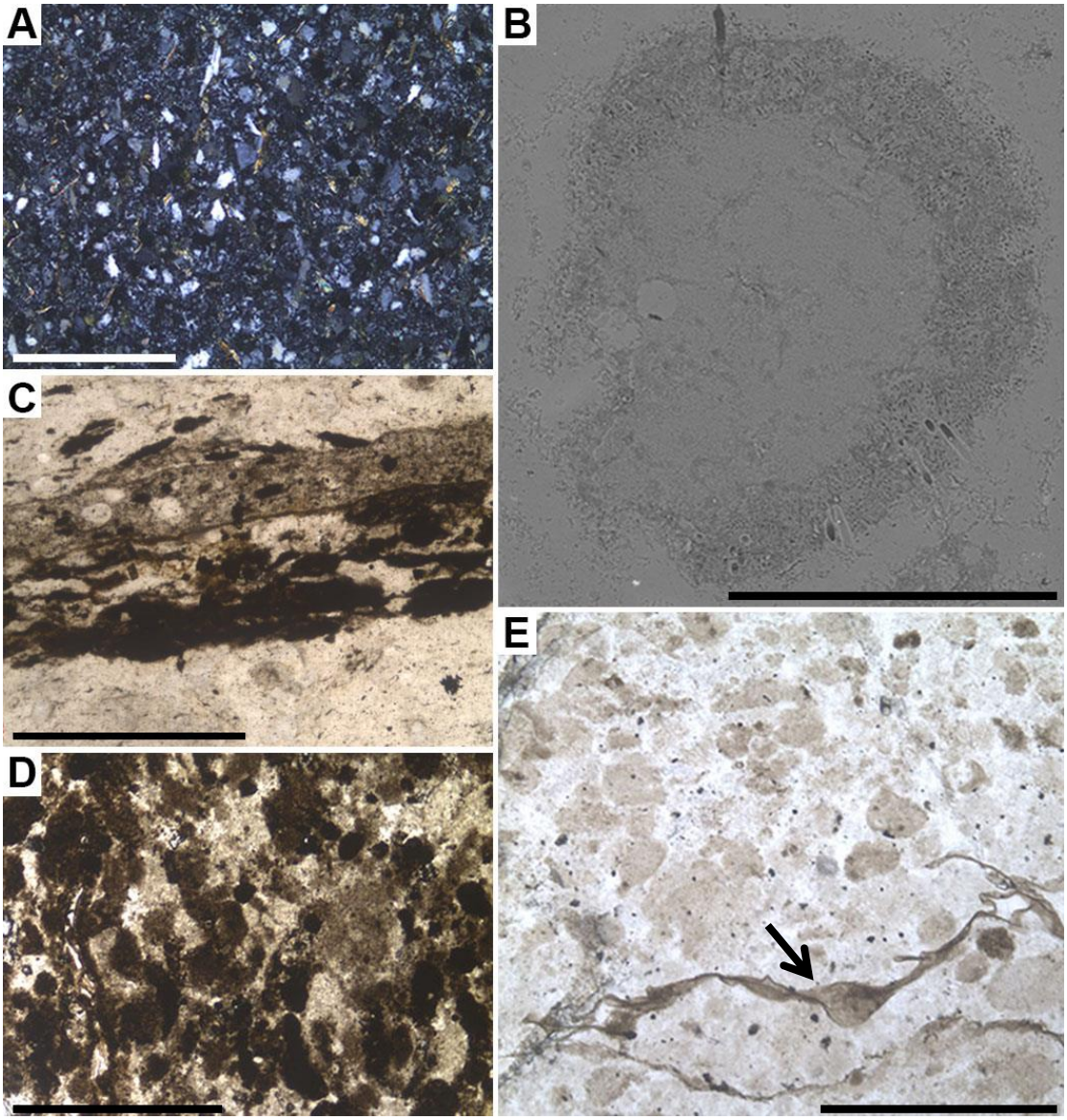

Figure 5. Transmitted light and SEM photomicrographs of lithology of the Yanjiahe Formation. Thin section numbers are followed by Olympus coordinates in parentheses. Scale bars equal 500 μm in A, C, D, and E; 200 μm in B.

A) Randomly oriented clay minerals (illite) and quartz silt in chert matrix, original lithology calcisiltite. 11-HZA-YJH-1.6 (18 × 129.8).

B) Secondary electron image of microbored siliceous grain. HZA-YJH-18.3.

C) Laminated peloidal packstone laminae and chert layers. 11-HZA-YJH-0.5 (12 × 116.7).

D) Peloidal packstone. GYE-16.5. (15.2 × 125.7).

E) Phosphoritic packstone containing abundant peloids in silicified micrite matrix, with a large smooth-walled acritarch (arrow). HZA-YJH-D (12.7 × 125.9).

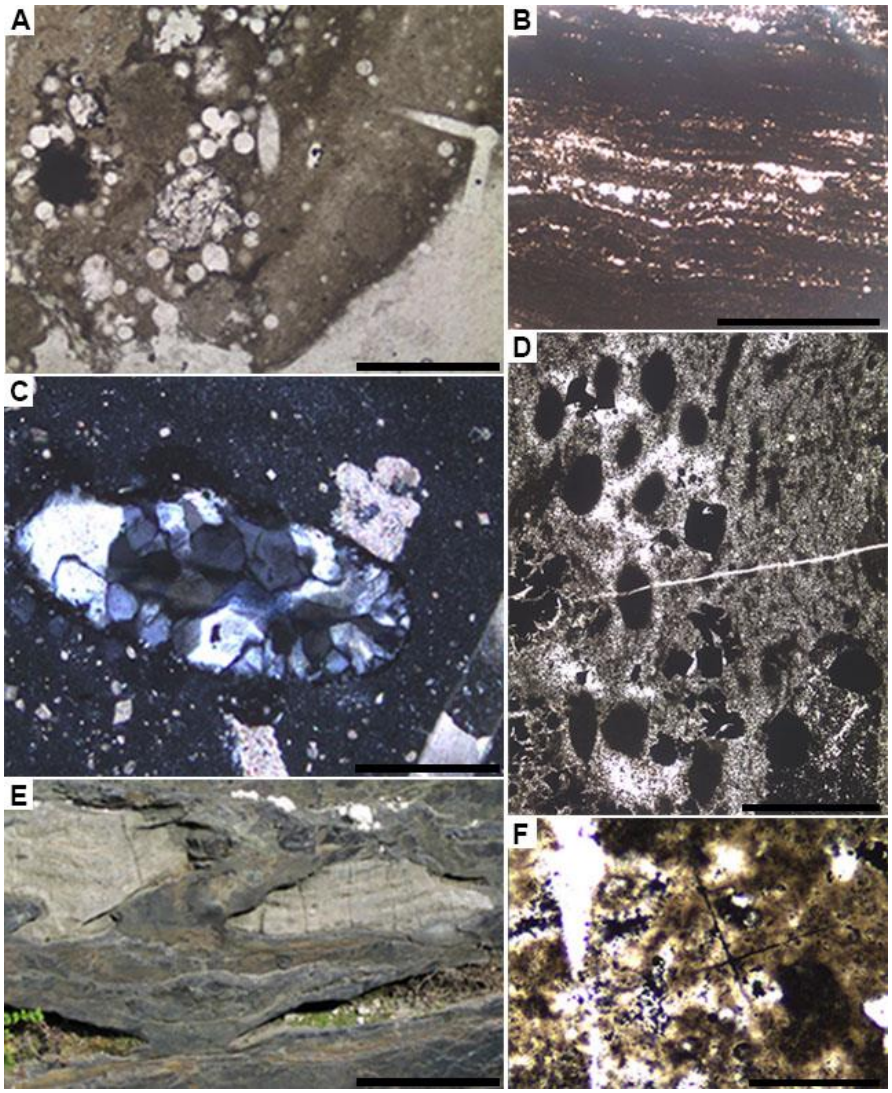

Figure 6. Transmitted light photomicrography and field photography of lithology of the Liuchapo Formation. Thin section numbers are followed by Olympus coordinates in parentheses. Scale bars equal 500 in for A & D; 200 μm in

B & C; 10 cm in E; 100 μm in F.

A) Spicular and phosphatic grains in silicified layer. 11-GZP-LCP-4.4. (16.5 × 117).

B) Polycrystalline quartz silt lithoclasts and anhedral carbonate crystals. 11-GZP-LCP-8.8. (5.2 × 119.7).

C) Wavy organic-rich laminations. 11-LYX-LCP-15.0 (14.5 × 131.5).

D) Rolled up Horodyskia in siliceous sediments. 11-GZP-LCP-4.4 (13.6 × 119.8)

E) Partially silicified soft-sediment deformation in outcrop, wavy to convoluted bedding. Ganziping, Hunan Province, South China.

F) Hexactinellid sponge spicule in phosphatic wackestone from the upper Liuchapo Formation, Longbizui. 11-LBZ-LCP-3.8. (20 × 115.7).

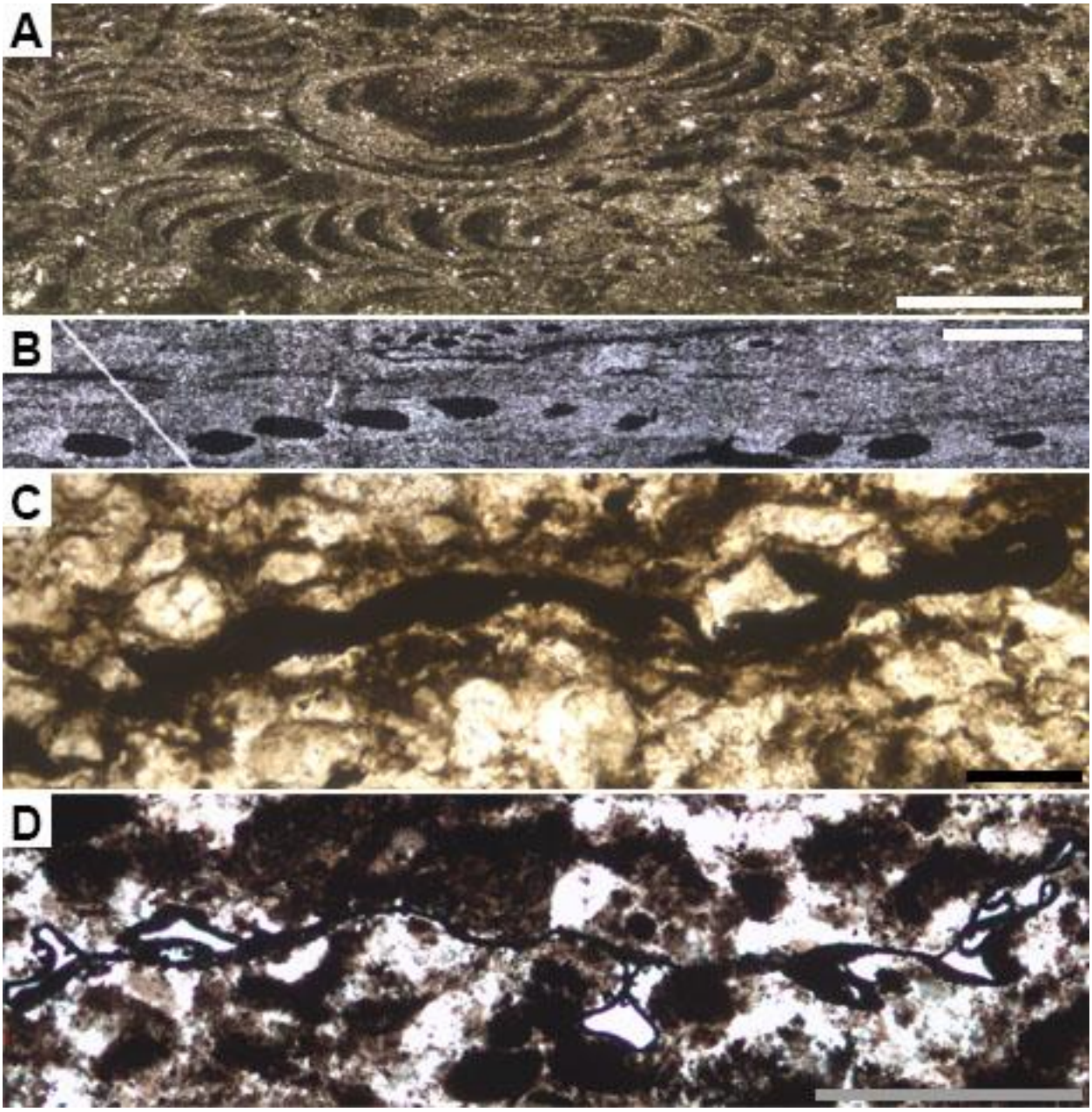

Figure 7. Transmitted light photomicrographs of HmPj assemblage fossils and *Leiosphaeridia* sp. Thin section numbers are followed by Olympus coordinates in parentheses. Scale bars are 100 μm.

A) *Palaeopascichnus jiumenensis*. Specimens are randomly oriented, some articulated. 11-GZP-LCP-0.6 (7.8 × 113.2).

B) *Horodyskia minor*. 11-SDP-LCP-11.0 (20 × 124).

C-D) Large, smooth-walled *Leiosphaeridia*. C) Ediacaran, 08-HZA-YJH-0.4 (9.0 × 136.8); D) Cambrian, 11-HZA-YJH-22.0 (13.5 × 112.1).

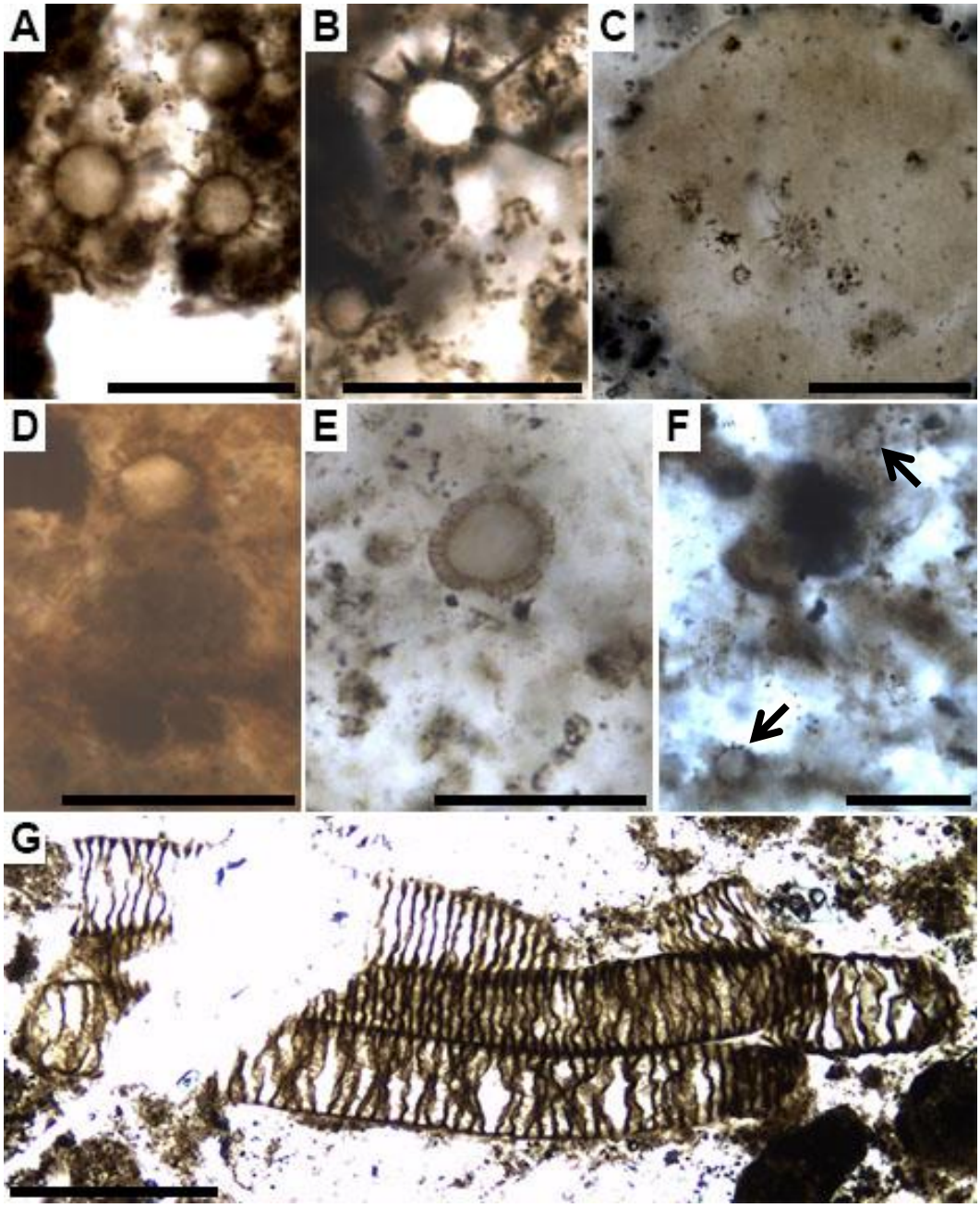

Figure 8. Transmitted light photomicrography of Cambrian acanthomorphic acritarchs and *Megathrix longus*. Thin section numbers are followed by Olympus coordinates in parentheses. Scale bars equal 20 μm in A &B; 50 μm in C & D; 30 μm in E & F; and 200 μm in G.

A-C) *Heliosphaeridium ampliatum*. A) 08-HZA-Cam-5.6 (16.2 × 138); B) 08-HZA-Cam-5.4 (10.6 × 123.9); C) 08-HZA-Cam-6.3 (10 × 146.5).

D-E) *Comasphaeridium annulare*. D) JQN-YJH-10.4 (8 × 125); E) JQN-YJH-10.5 (8 × 125.7).

F) *Asteridium tornatum* (arrows). JQN-YJH-9.8 (5.6 × 137.4).

G) *Megathrix longus*. 08-HZA-Cam-6.3 (19.2 × 127).

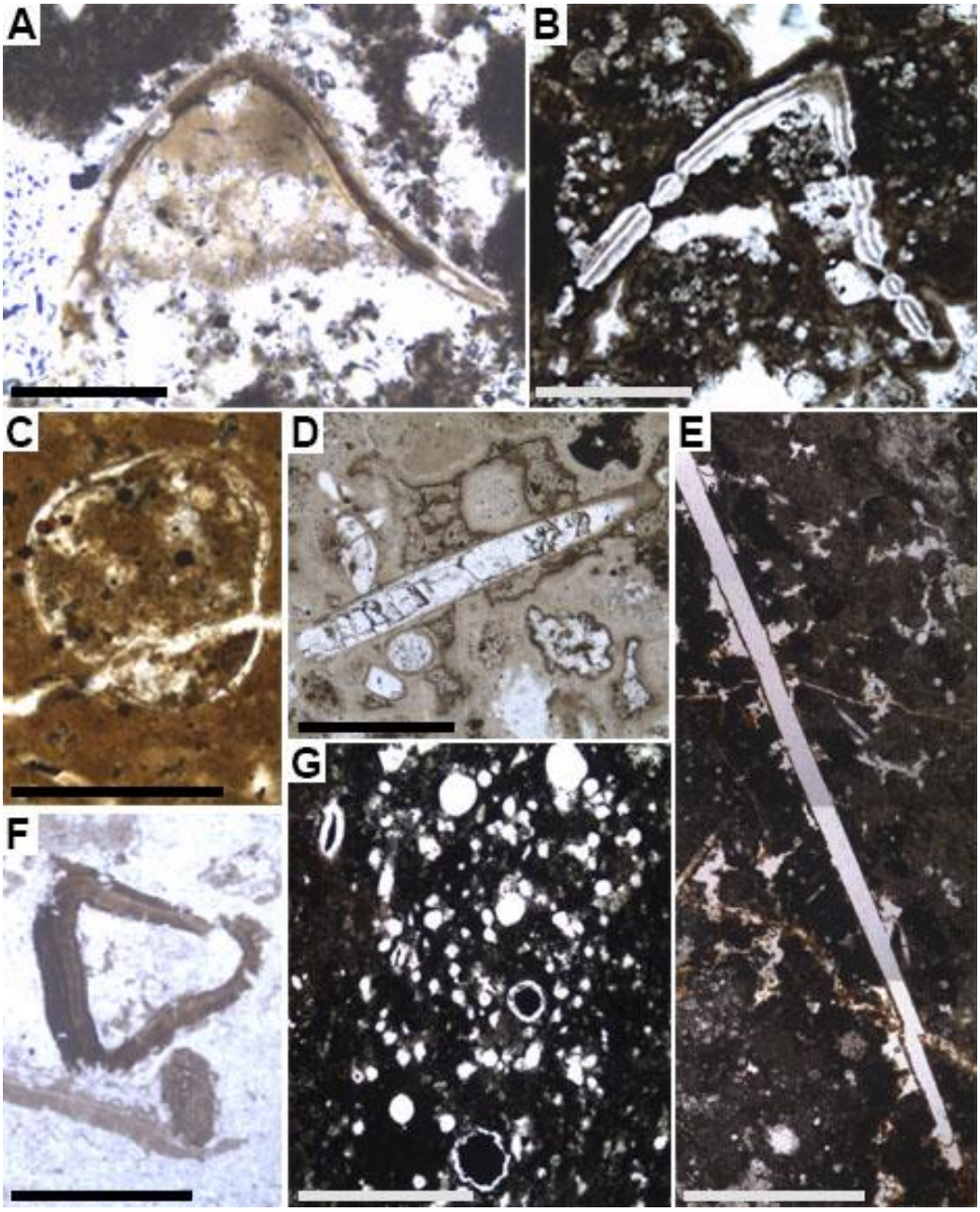

Figure 9. Transmitted light photomicrography of Cambrian small shelly fossils. Thin section numbers are followed by Olympus coordinates in parentheses. Scale bar equals 200 μm for A-E; and 500 μm for F & G.

A & B. *Kaiyangites novilis*. A) 08-HZA-Cam-6.3 (4.7 × 137.7). B) 08-HZA-Cam-6.3 (17.8 × 126.4).

C. *Anabarites trisulcatus*. 11-JPY-YJH-F-a (5.4 × 126.1).

D, E, G. Disarticulated sponge spicules. D) HZA-YJH-0.5 (16.6 × 108); E) 11-SC-NTT-0.7 (17 × 125); G) 11-LBZ-NTT-0.7 (19 × 136.6).

F. Triangular small shelly fossil. 11-BGT-YJH-0.01b (10.1 × 125).

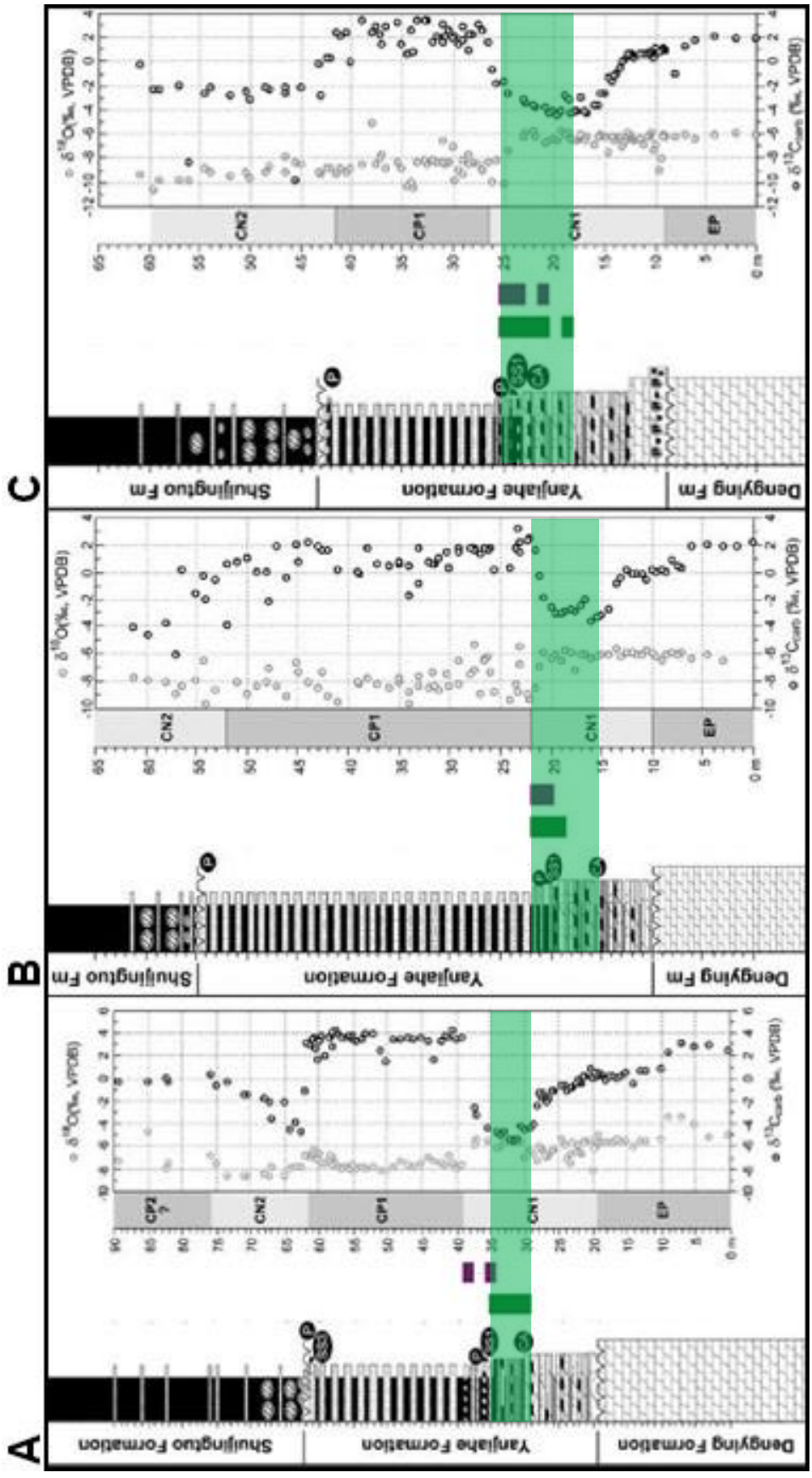

Figure 10. Correlation of Cambrian small shelly fossils with the basal Cambrian carbon isotope excursion.(Jiang et al., 2012). Data from the current study are represented by the thick vertical bars next to the stratigraphic column. Green bars = AHC-bearing strata, Purple bars = SSF-bearing strata. Highlighted strata reveal consistent match of AHC range with negative carbon isotope excursion. CA = Cambrian acritarchs, SSF = Small shelly fossils, P = clastic chert-phosphate layer, T = Trilobites.

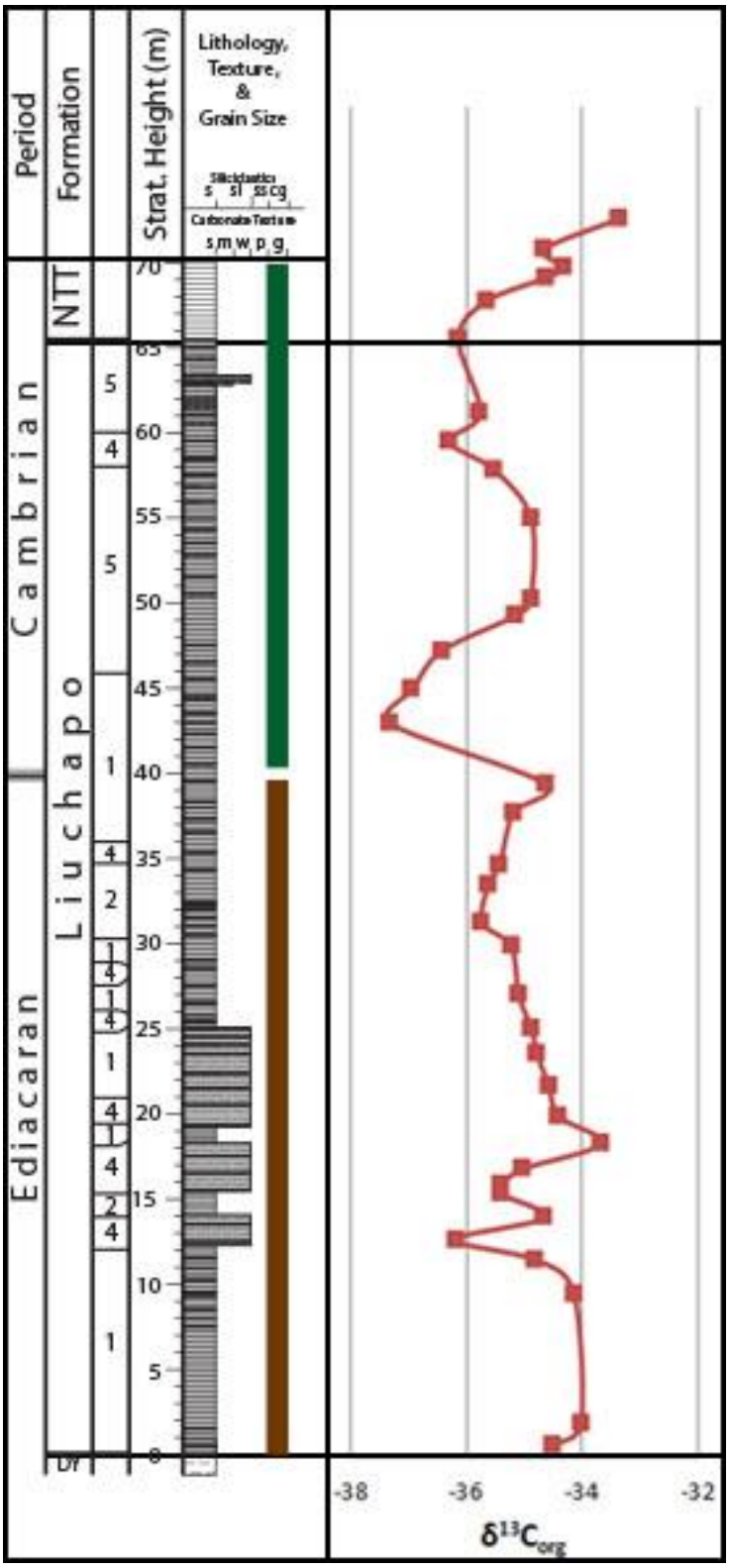

Figure 11. Comparative organic carbon isotope stratigraphy and HmPj-AHC biostratigraphy. The Ediacaran-Cambrian boundary defined from biostratigraphy coincides with a negative isotope shift interpreted as a chemostratigraphic proxy for the boundary by Wang et al. (2012a).

Appendix

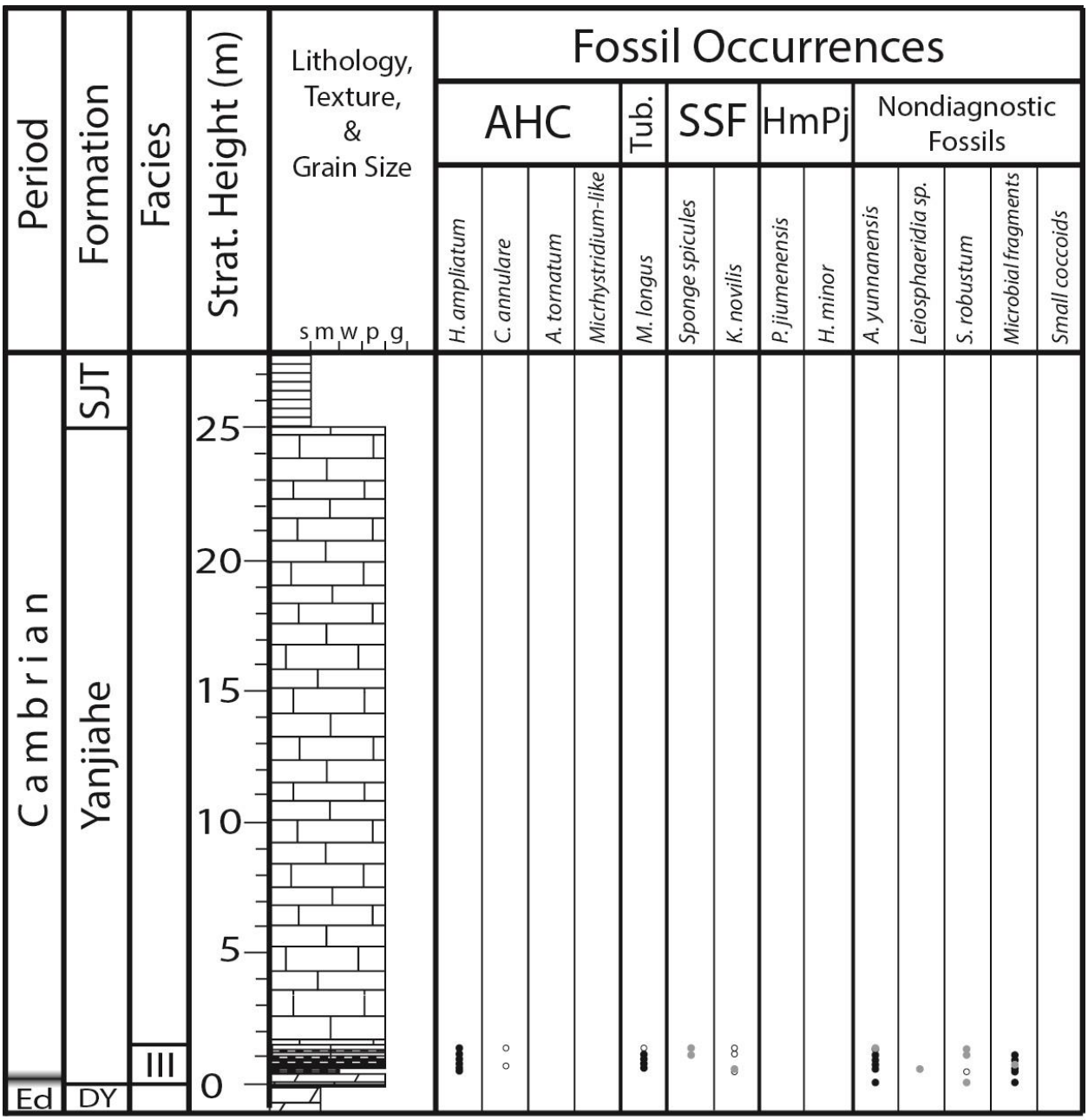

Appendix1. Lithostratigraphic column and fossil distributions of the Yanjiahe Formation at Baiguotang (innermost shelf).

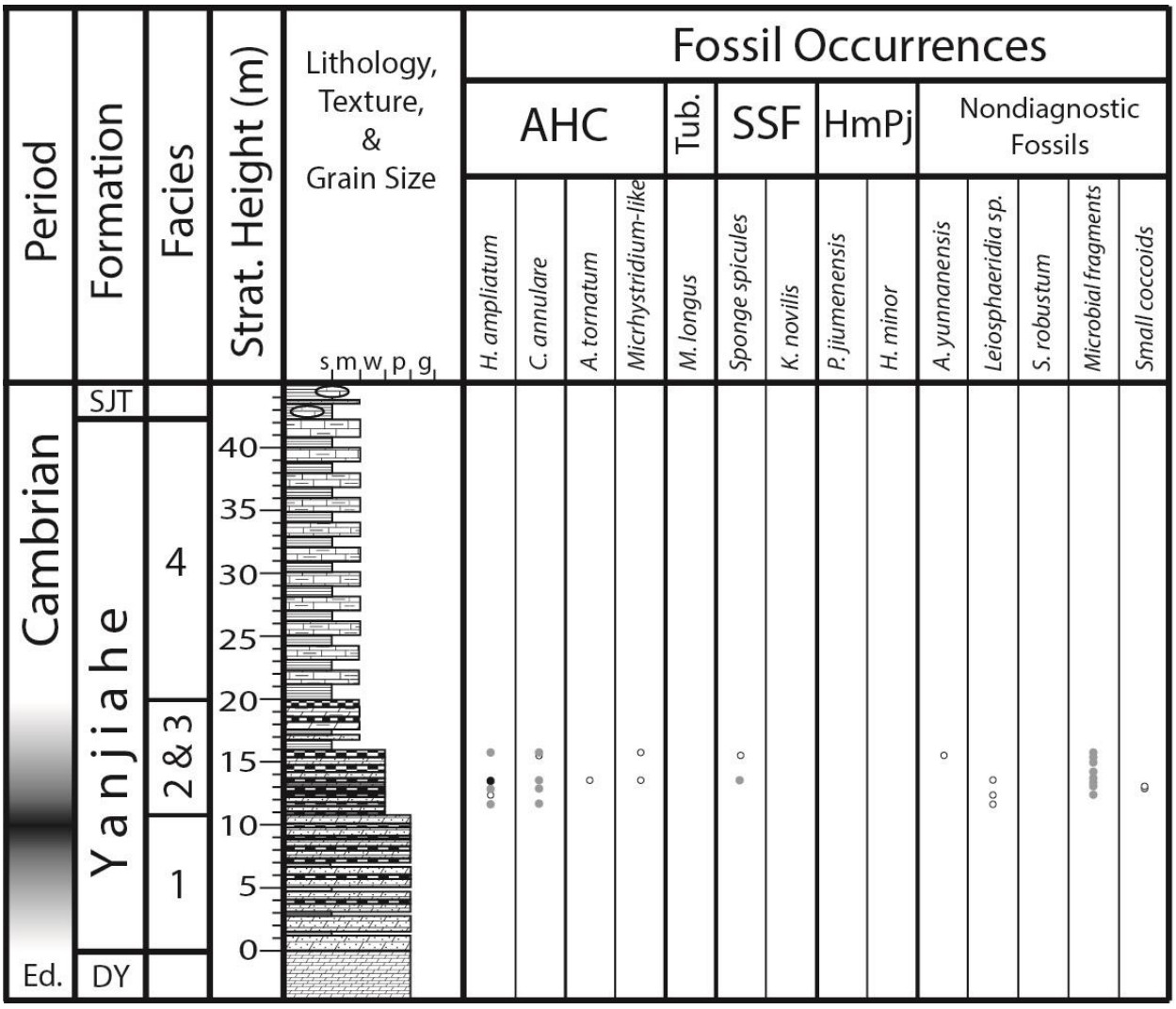

Appendix 2. Lithostratigraphic column and fossil distributions of the Yanjiahe Formation at Jijiapo.

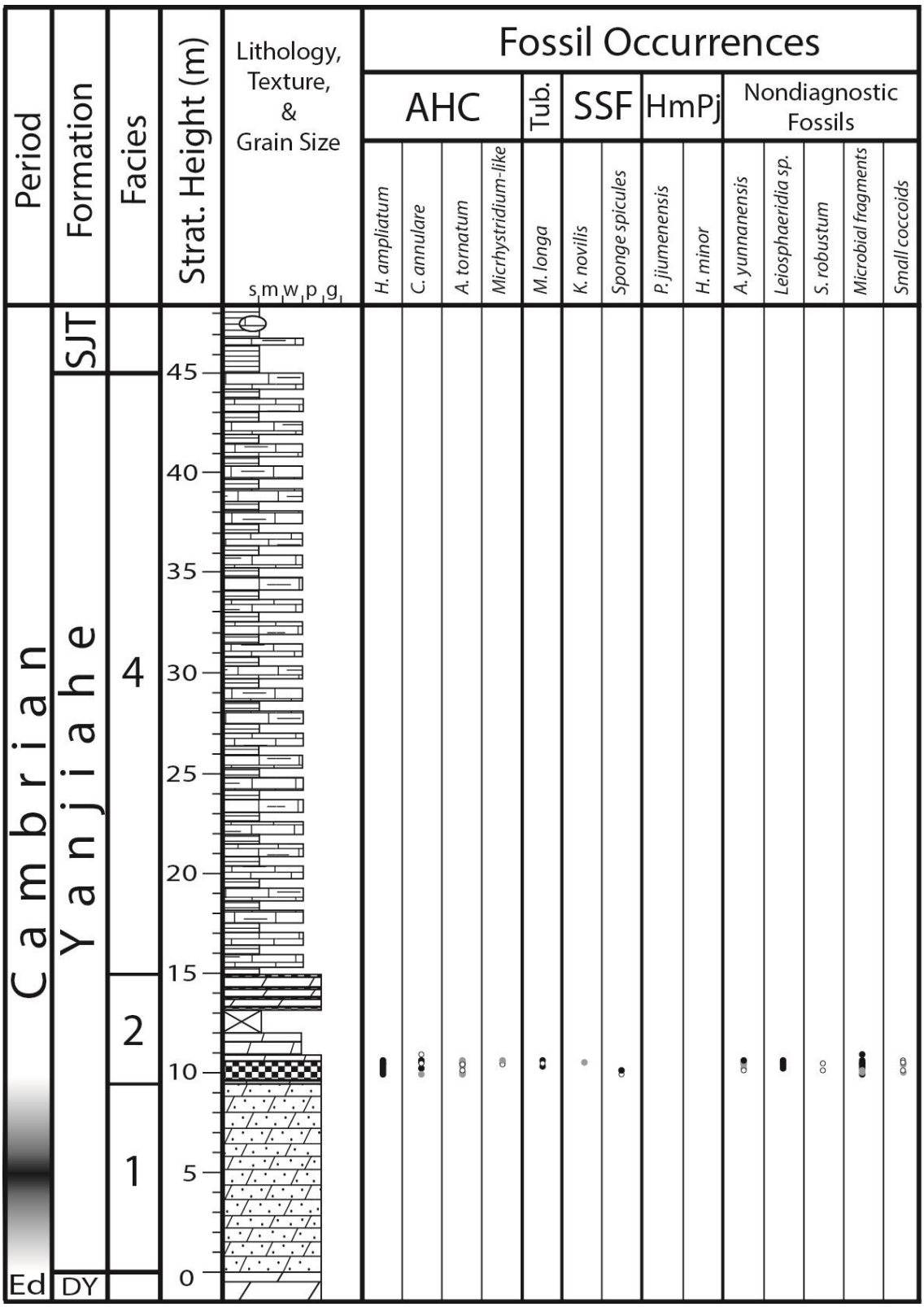

Appendix 3. Lithostratigraphic column and fossil distributions of the Yanjiahe Formation at Jiuqunao.

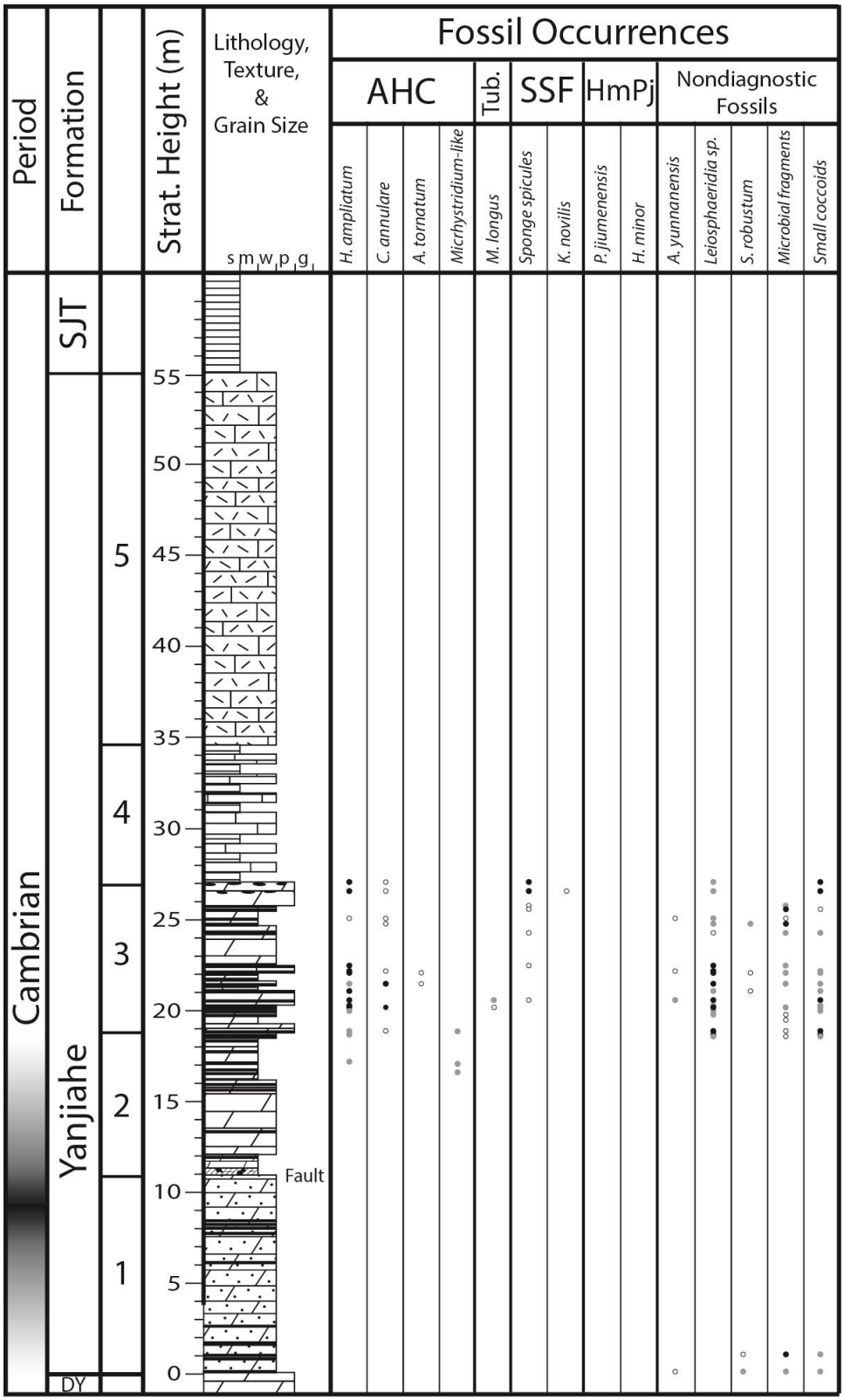

Appendix 4. Lithostratigraphic column and fossil distributions of the Yanjiahe Formation at Hezi'ao.

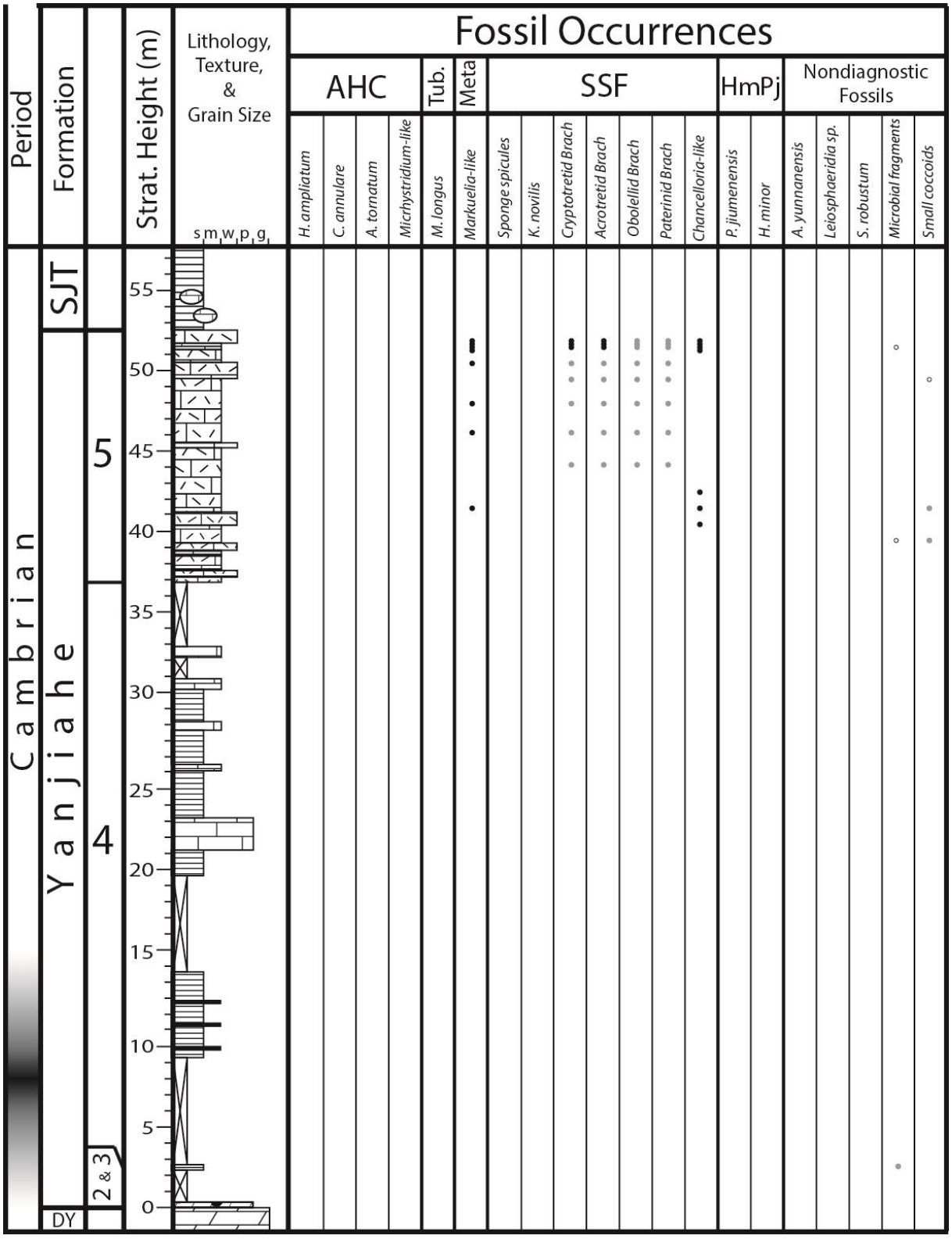

Appendix 5. Lithostratigraphic column and fossil distributions of the Yanjiahe Formation at Wangzishi.

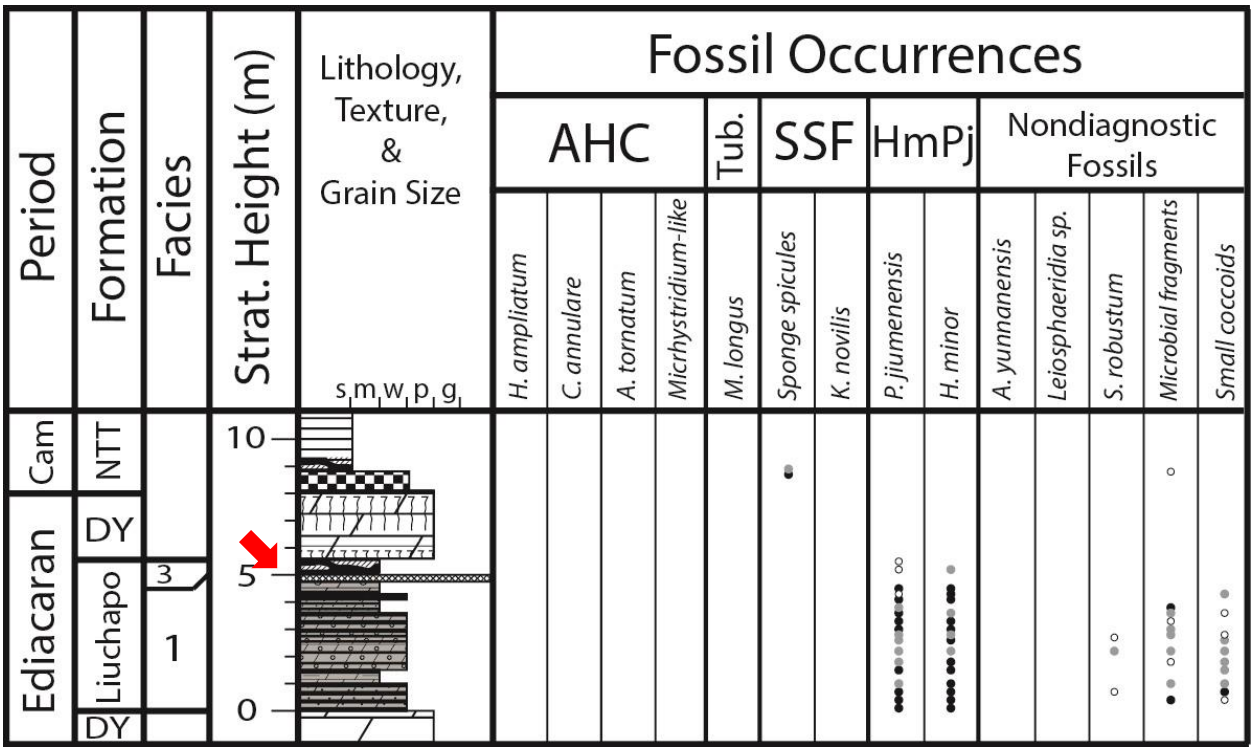

Appendix 6. Lithostratigraphic column and fossil distributions of the Liuchapo and Niutitang formations at Ganziping. Ash bed dated to 536.3 ± 5.5 Ma (Chen et al., 2009).

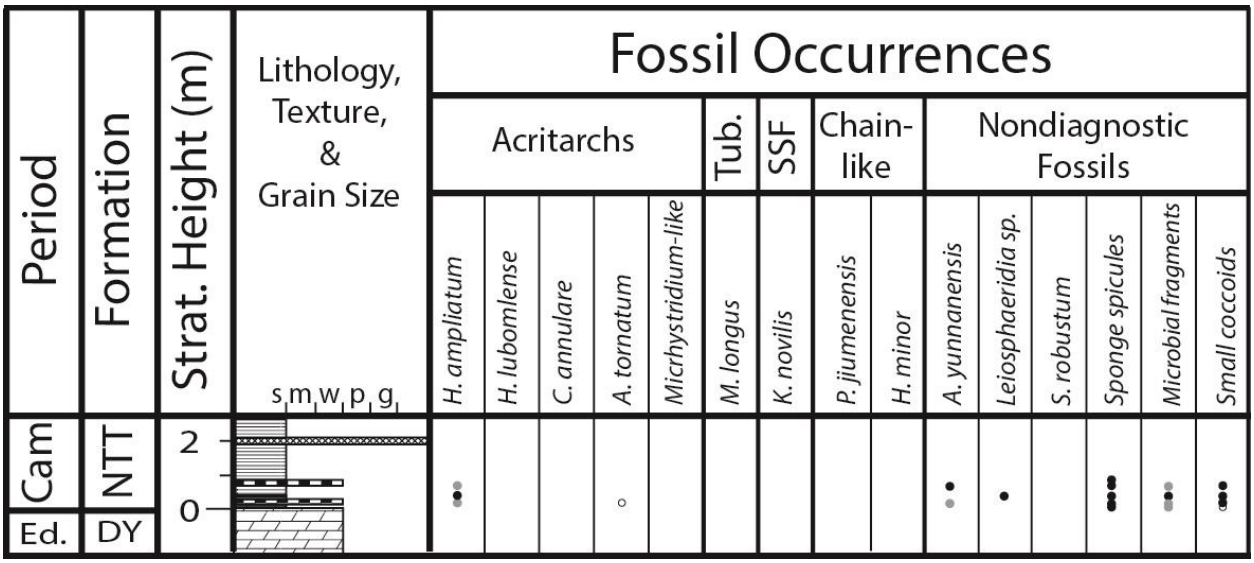

Appendix 7 Lithostratigraphic column and fossil distributions of the Niutitang Formation at Sancha.

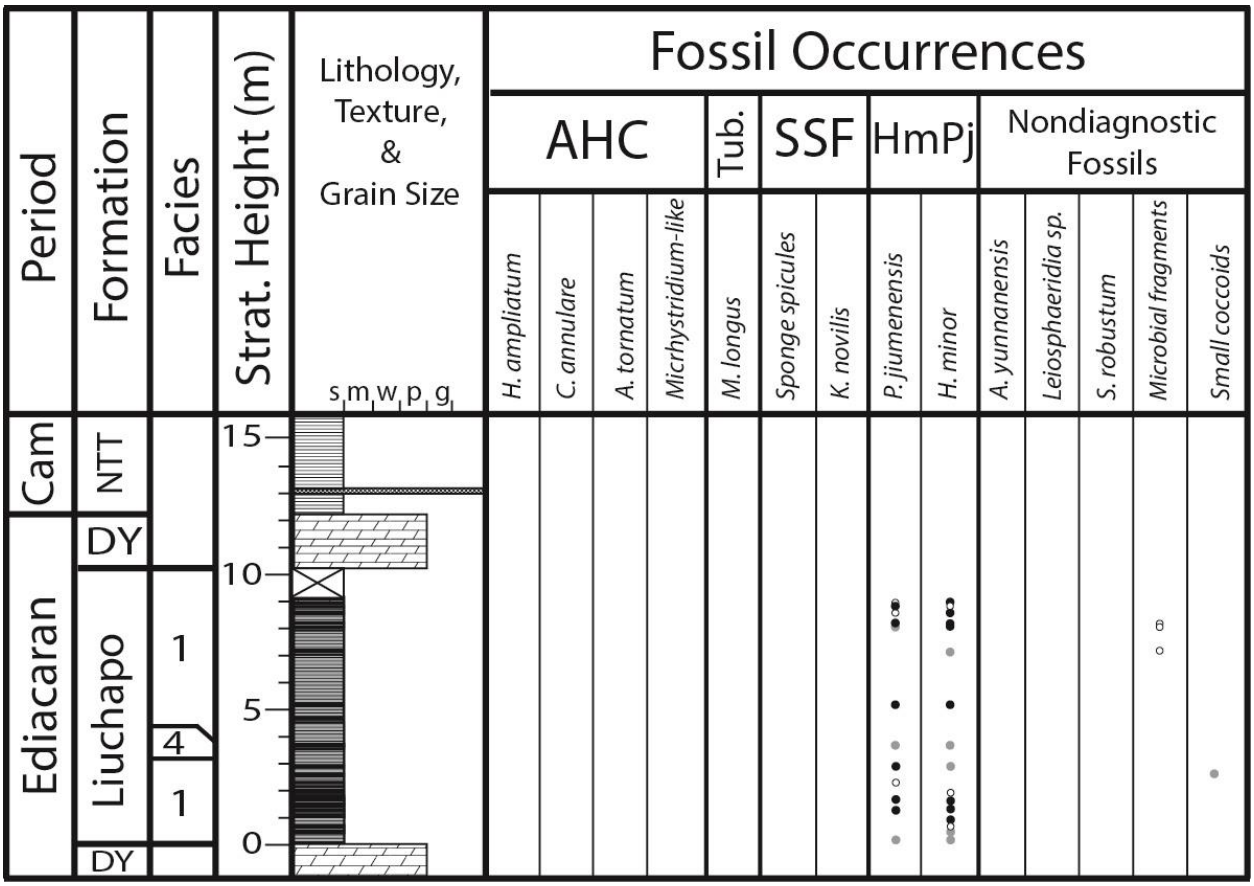

Appendix 8. Lithostratigraphic column and fossil distributions of the Liuchapo and Niutitang formations at Daping.

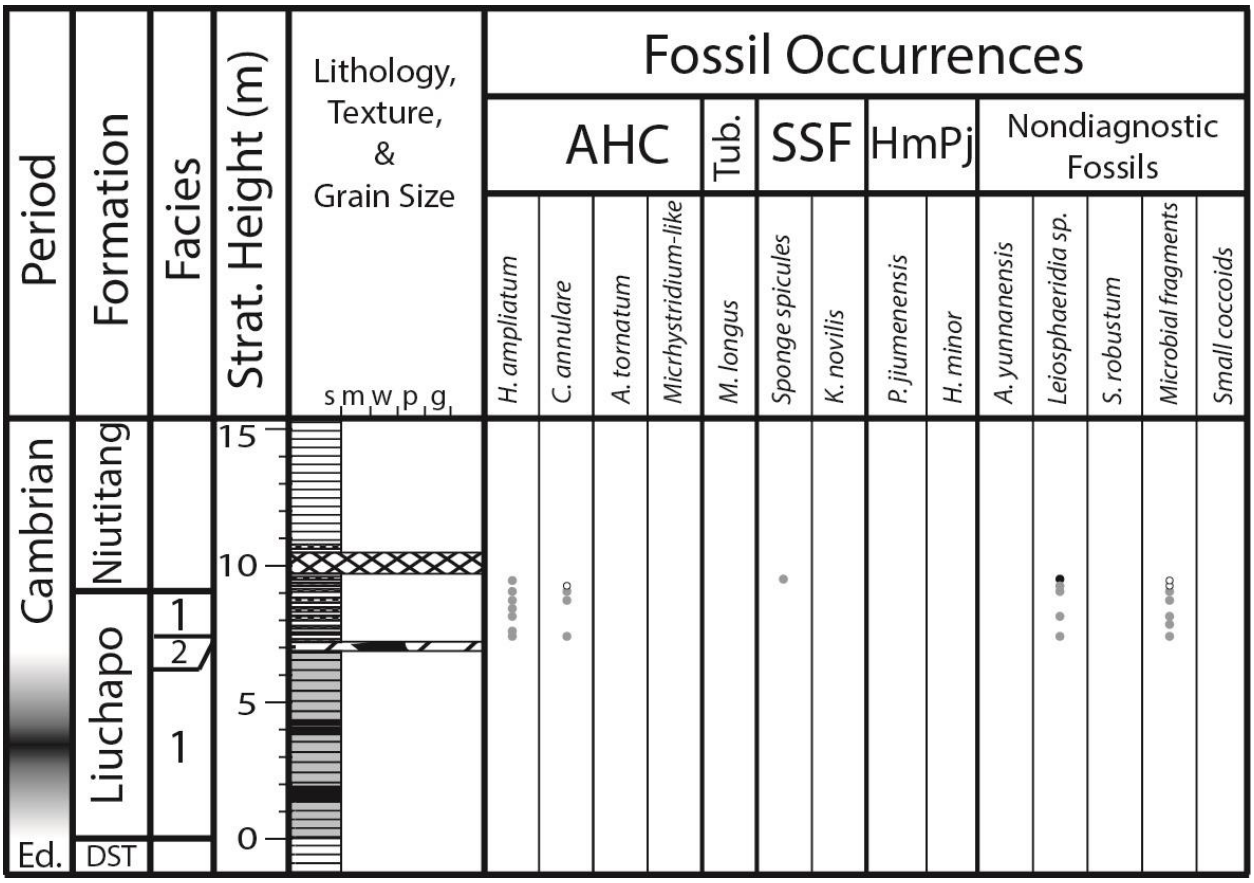

Appendix 9. Lithostratigraphic column and fossil distributions of the Liuchapo and Niutitang formations at Taoying.

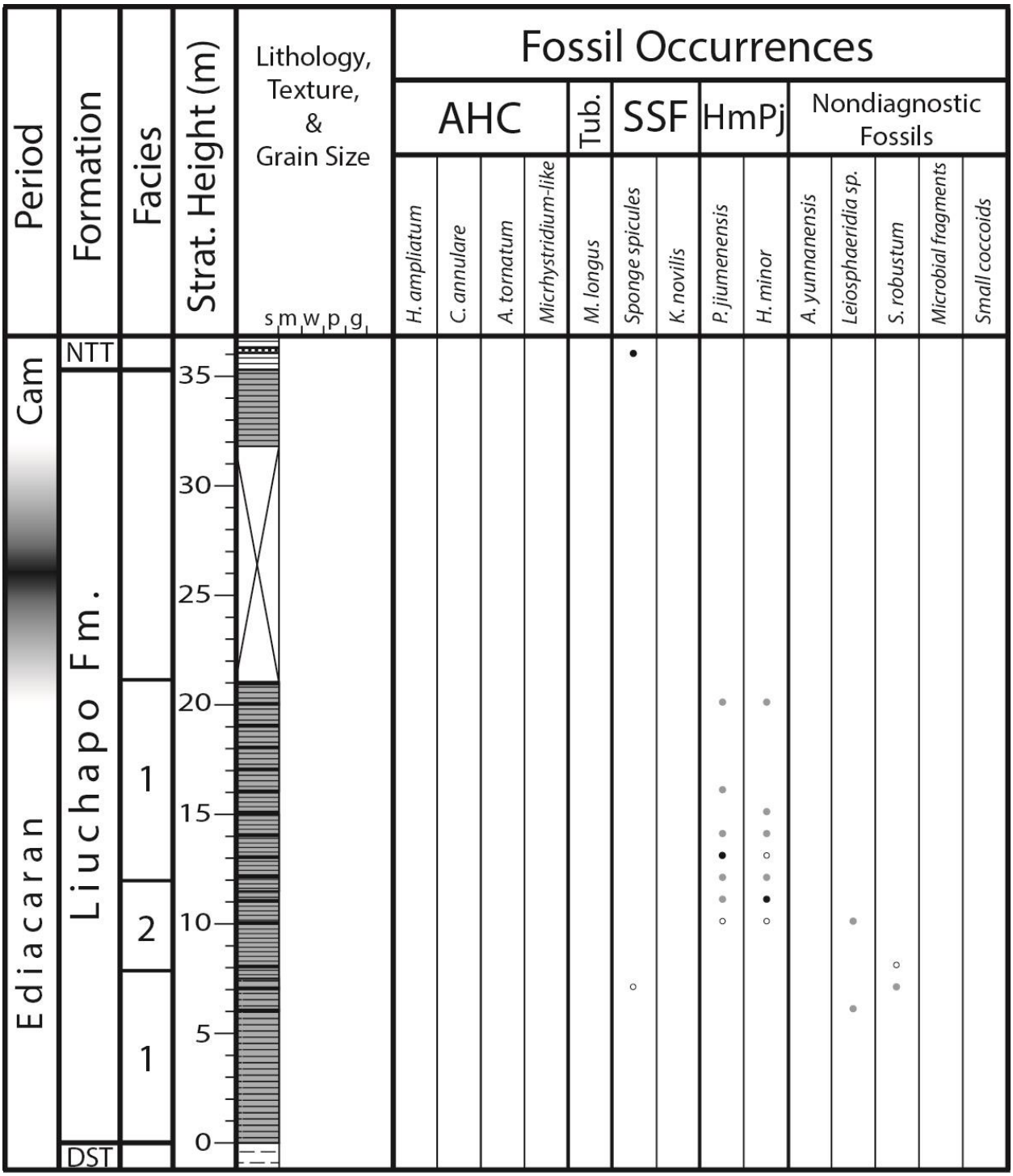

Appendix 10. Lithostratigraphic column and fossil distributions of the Liuchapo Formation at Siduping.

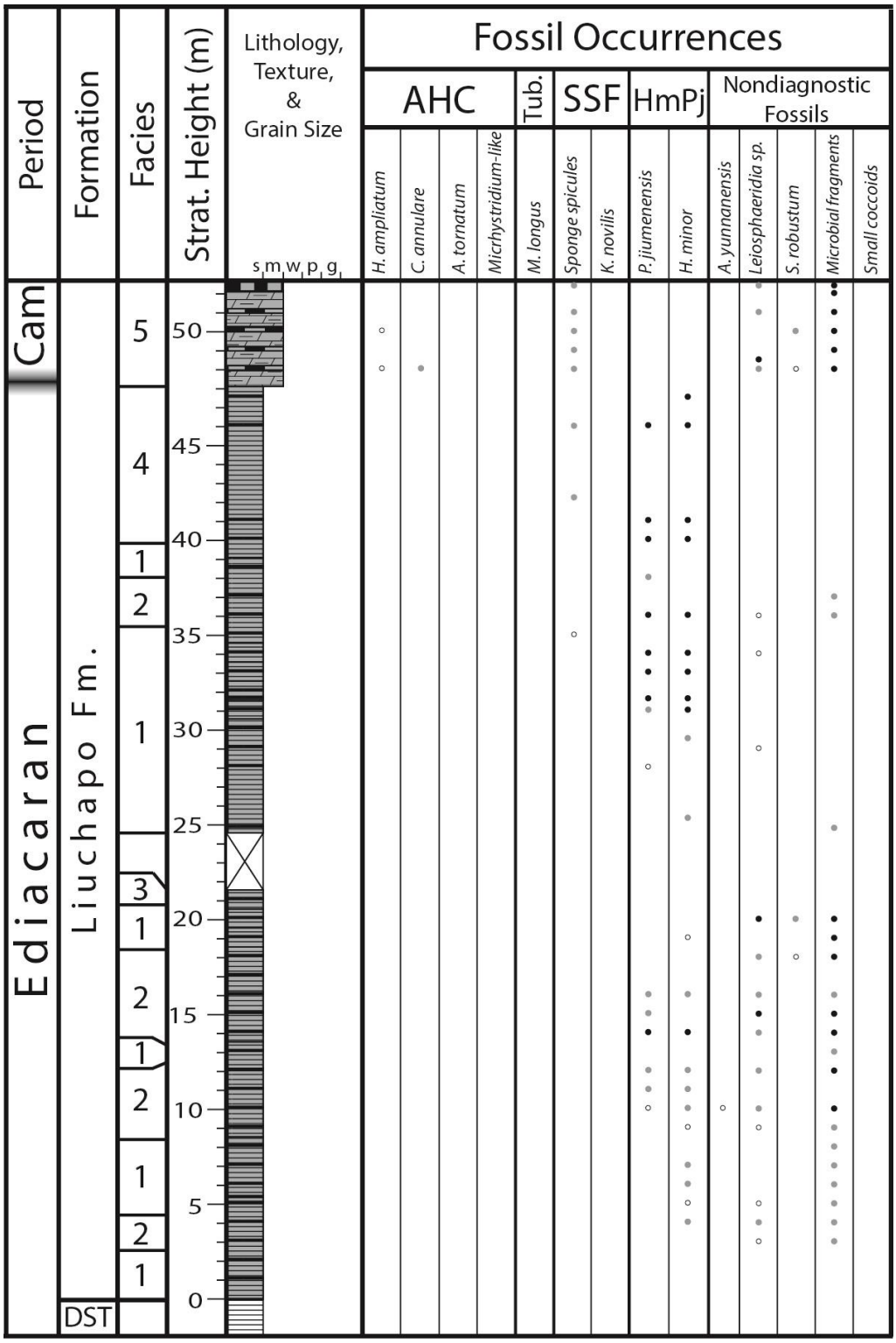

Appendix 11. Lithostratigraphic column and fossil distributions of the Liuchapo Formation at Xugongping.

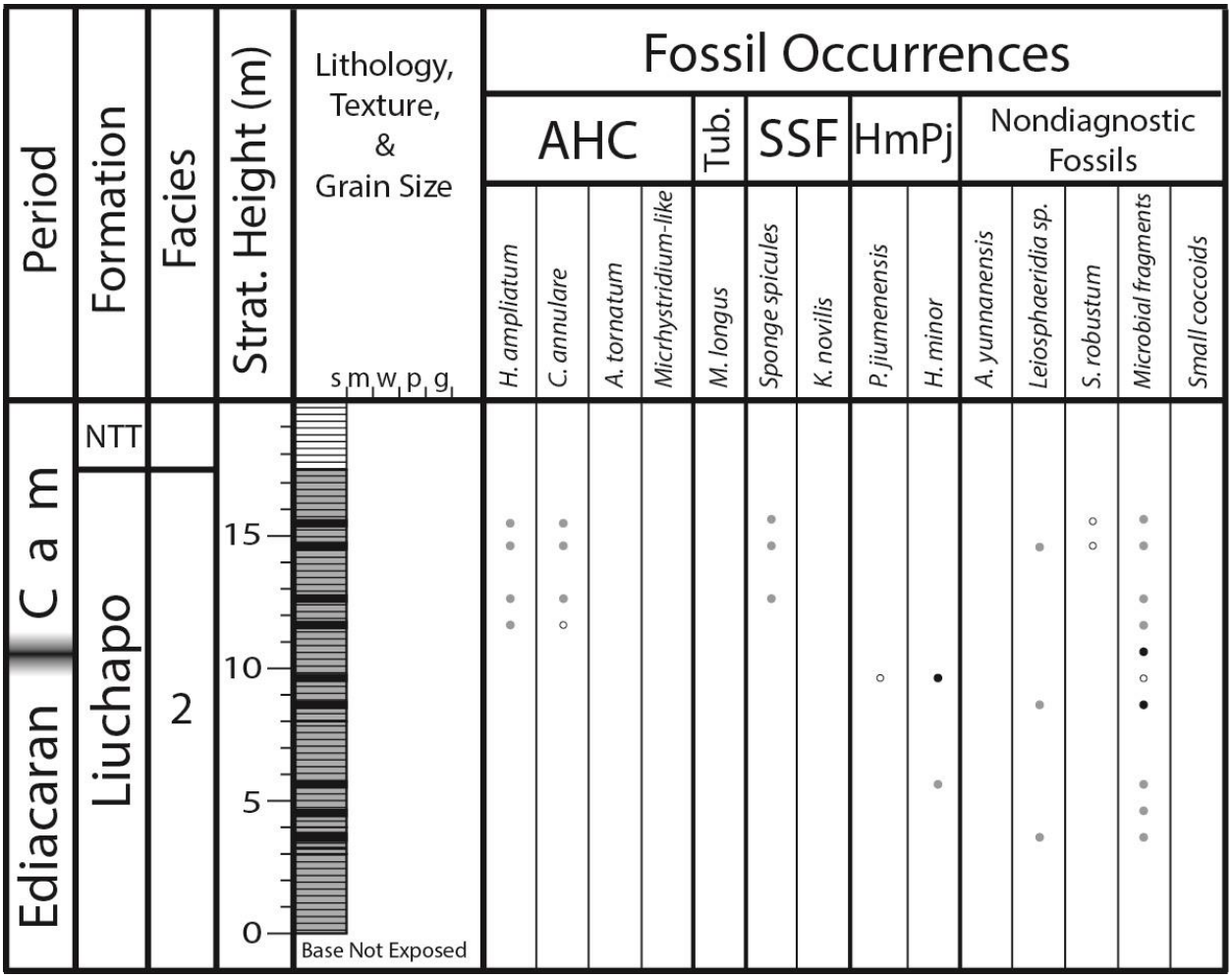

Appendix 12. Lithostratigraphic column and fossil distributions of the Liuchapo Formation at Louyixi.

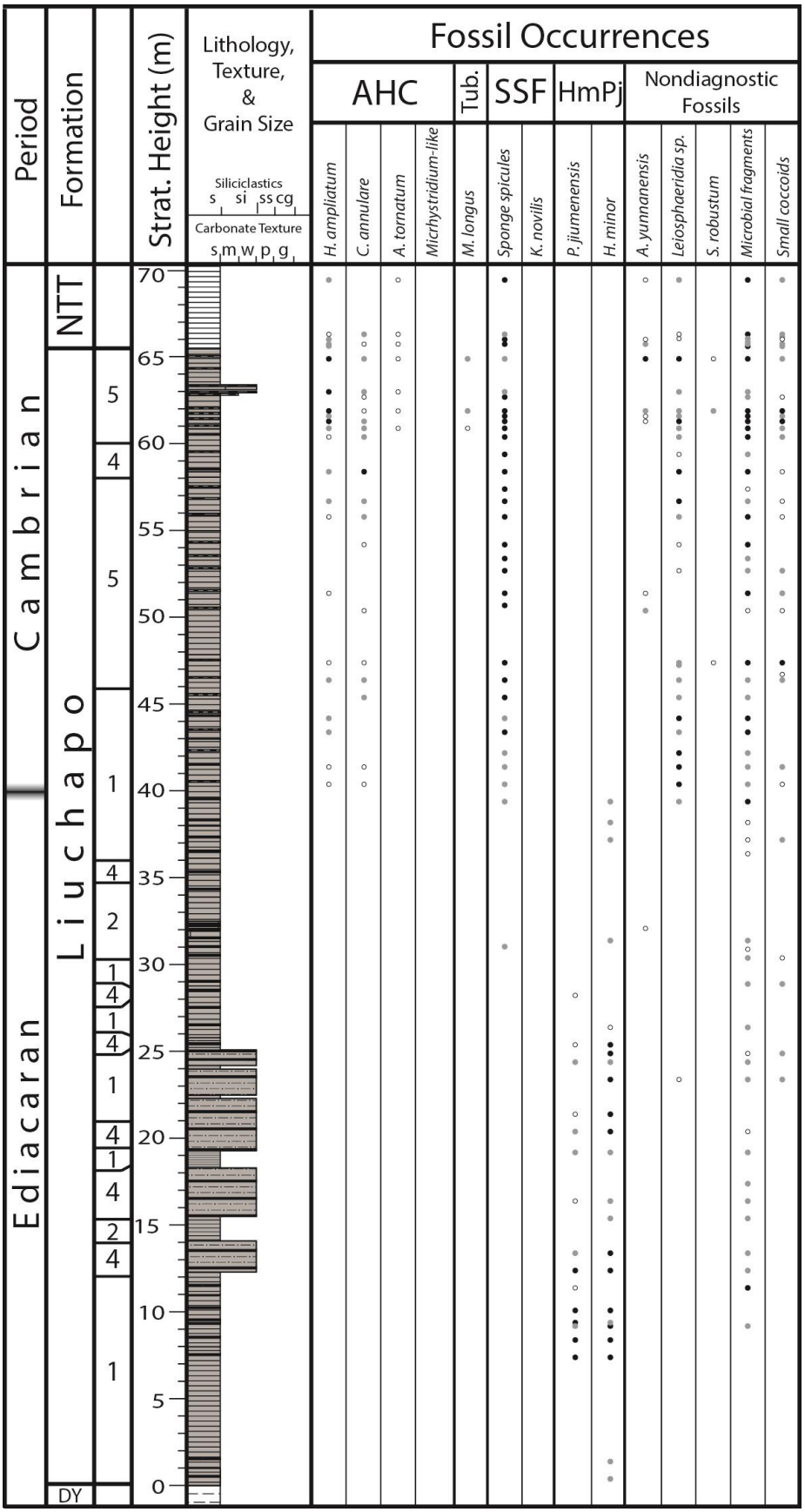
Period
Formation
Strat. Height (m)
Lithology, Texture, & Grain Size
Siliciclastics
s si ss cg
Carbonate Texture
s m w p g
Fossil Occurrences
AHC
Tub.
SSF
HmPj
Nondiagnostic Fossils
H. ampliatum
C. annulare
A. tornatum
Micrhystridium-like
M. longus
Sponge spicules
K. novilis
P. jiumenensis
H. minor
A. yunnanensis
Leiosphaeridia sp.
S. robustum
Microbial fragments
Small coccoids
Ediacaran
Cambrian
Liuchapo
NTT
DY
70
65
60
55
50
45
40
35
30
25
20
15
10
5
0

Appendix 13. Lithostratigraphic column and fossil distributions of the Liuchapo and Niutitang formations at Longbizui.

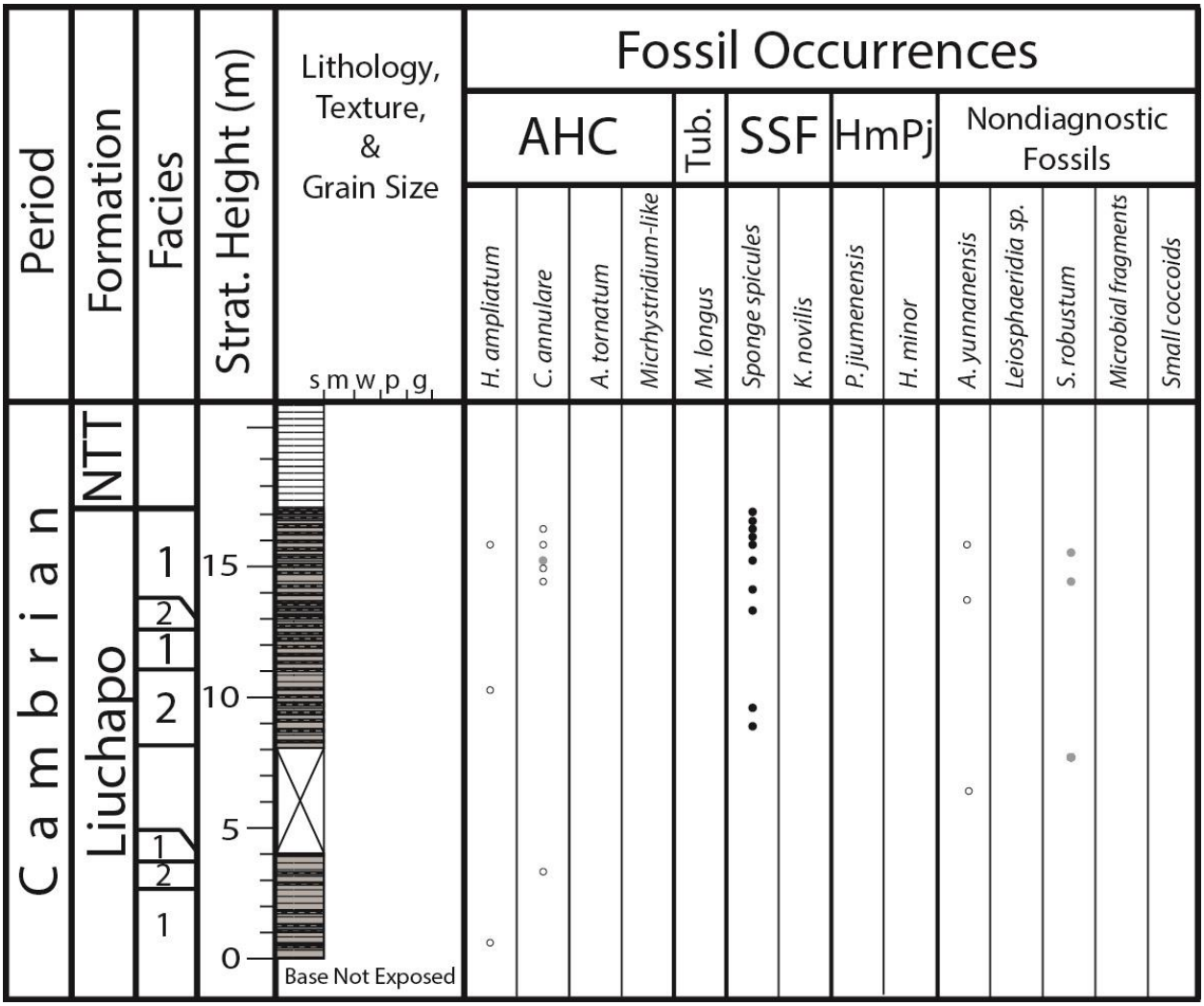

Appendix 14. Lithostratigraphic column and fossil distributions of the Liuchapo Formation at Yanwutan.

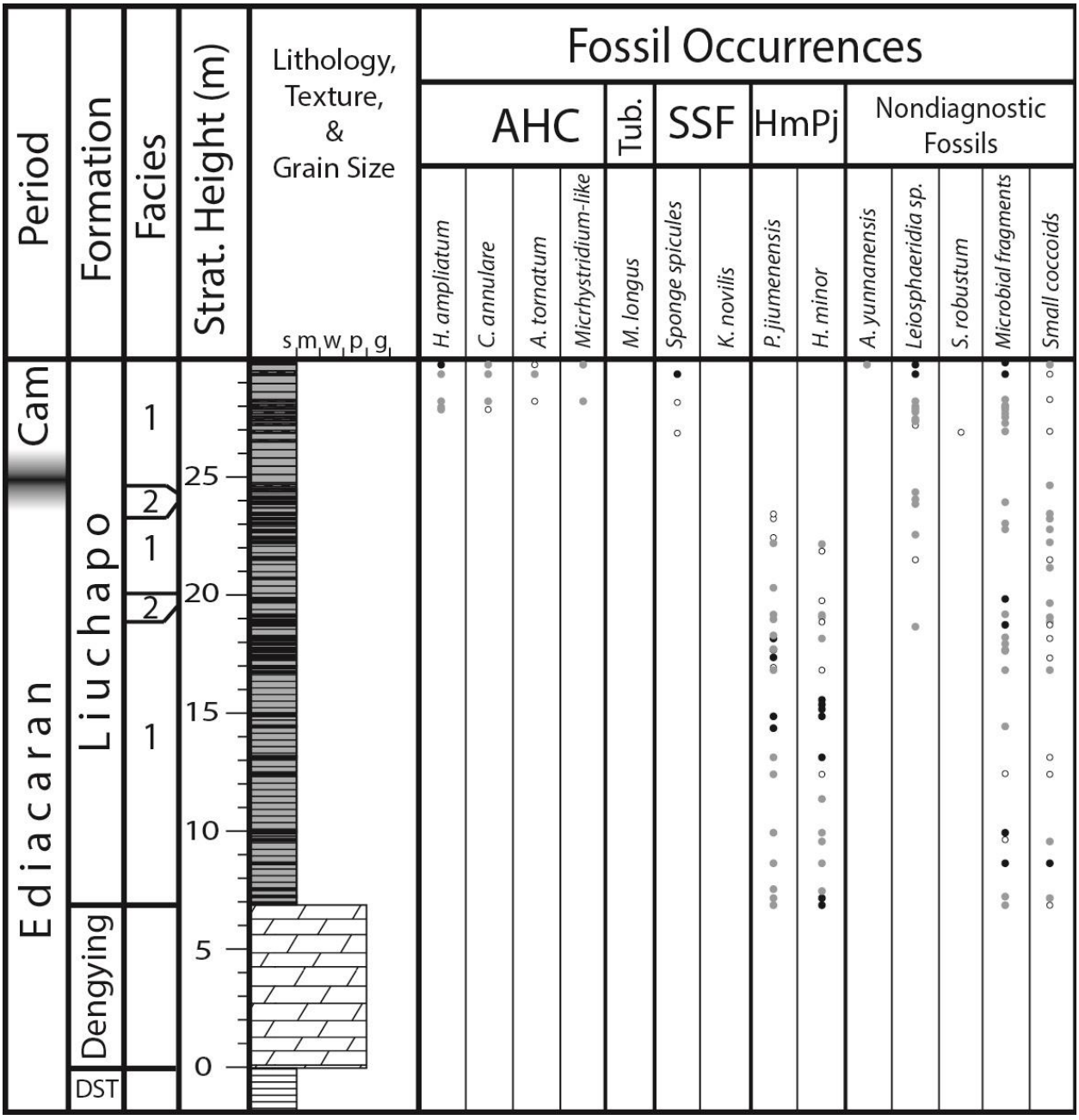

Appendix 15. Lithostratigraphic column and fossil distributions of the Liuchapo Formation at Jianxincun.